ANL/FPP-77-7

ANL/FPP-77-7

FUSION POWER PROGRAM
QUARTERLY PROGRESS REPORT

October–December 1977

U of C-AUA-USDOE

ARGONNE NATIONAL LABORATORY, ARGONNE, ILLINOIS

Prepared for the U. S. DEPARTMENT OF ENERGY
under Contract W-31-109-Eng-38

DISCLAIMER

Printed in the United States of America
Available from
National Technical Information Service
U. S. Department of Commerce
5285 Port Royal Road
Springfield, Virginia 22161
Price: Printed Copy $~~6.00~~ 5.25; Microfiche $3.00

Distribution Categories:
UC-20, -20a, -20b, -20c,
-20d, -20e, -20f, -20g

ANL/FPP-77-7

ARGONNE NATIONAL LABORATORY
9700 South Cass Avenue
Argonne, Illinois 60439

04388

FUSION POWER PROGRAM QUARTERLY PROGRESS REPORT

October—December 1977

Charles C. Baker, Director
Joseph B. Darby, Jr., Associate Director
Samuel D. Harkness, Associate Director

FOREWORD

This quarterly report describes fusion-related activities in research, development and reactor design and analysis conducted within the Fusion Power Program and within other programs at Argonne National Laboratory.

Previous quarterly reports issued were:

CTR/TM-11	January-March 1974
CTR/TM-24	April-June 1974
CTR/TM-29	July-September 1974
CTR/TM-38	October-December 1974
ANL/CTR/TM-39	January-March 1975
ANL/CTR/TM-45	April-June 1975
ANL/CTR-75-3	July-September 1975
ANL/CTR-75-5	October-December 1975
ANL/CTR-76-2	January-March 1976
ANL/CTR-76-4	April-June 1976
ANL/CTR-76-5	July-September 1976
ANL/FPP-76-6	October-December 1976
ANL/FPP-77-1	January-March 1977
ANL/FPP-77-2	April-June 1977
ANL/FPP-77-4	July-September 1977

TABLE OF CONTENTS

TABLE OF CONTENTS (Continued)

LIST OF FIGURES

LIST OF FIGURES (Continued)

LIST OF TABLES

(1-33)

04389

I. FUSION REACTOR MATERIALS

A. Plasma Materials Interactions

1. Depth Distribution of Bubbles in 20-keV $^4He^+$ Irradiated-Nickel

G. Fenske, S. K. Das, M. Kaminsky, Physics Division, and
G. H. Miley*

Helium blistering can become an important surface erosion process during the operation of fusion reactors. However, the mechanism of blister formation is still not well understood.[1] Our studies[2] of the depth distribution of helium bubles are aimed at obtaining a better understanding of the blistering phenomenon. Particularly, we want to understand the experimental observation[1] that the blister skin thickness values for many metals irradiated with He^+ ions of energies lower than 20-keV are a factor of two or more larger than the calculated projected ranges. In the present paper, the depth distribution of helium bubbles obtained from transmission electron microscopy (TEM) are compared with the theoretical projected range and damage-energy distributions.

Polycrystalline nickel foils ($\sim$ 0.002" thick) of 99.995% purity (Marz grade) were obtained from Material Research Corporation. The foils were first metallographically polished, then annealed at 900°C for two hours in a vacuum of $\sim 1 \times 10^{-7}$ torr and finally electropolished in a solution containing 140 ml phosphoric acid, 10 ml H_2SO_4, 43 ml H_2O and 2 g chromium trioxide. The targets were irradiated at 500°C in a vacuum of $\sim 1 \times 10^{-8}$ torr with 20-keV $^4He^+$ ions. The irradiated foils were first lightly sputter cleaned with 2-keV Ar^+ ions, then given a nickel strike and finally electroplated with nickel. The electroplated samples were then sectioned parallel to the direction of the incident beam and 3 mm discs were spark cut from them. Thin foils suitable for TEM were prepared by electrolytic jet polishing. This novel transverse sectioning technique allows one to study the entire depth distribution of bubbles from a single specimen. Some variation of this technique has been used to study the depth distribution of damage[3] and of voids[4] but for gas bubbles, only conventional techniques have been used.[5]

Figure I-1(a), I-1(b) and I-1(c) show typical transmission electron micrographs of the plated and irradiated regions for annealed polycrystalline

---

* University of Illinois, Urbana, Illinois.

1 S. K. Das and M. Kaminsky, Adv. in Chemistry, 158, 112 (1976).

2 G. Fenske, S. K. Das, M. Kaminsky, Bull. Amer. Phys. Soc. 22, 380 (1977).

3 J. Narayan, O. S. Oen and T. S. Noggle, J. Nucl. Mat. 71, 160 (1977).

4 J. B. Whitley, P. Wilkes and G. L. Kulcinski, Trans. ANS, 23, 136 (1976).

5 K. Ehrlich and D. Kaletta, Proc. Int. Conf. on Radiation Effects and Tritium Technology for Fusion Reactors, CONF-750989 Vol. II, p. 289 (1976).

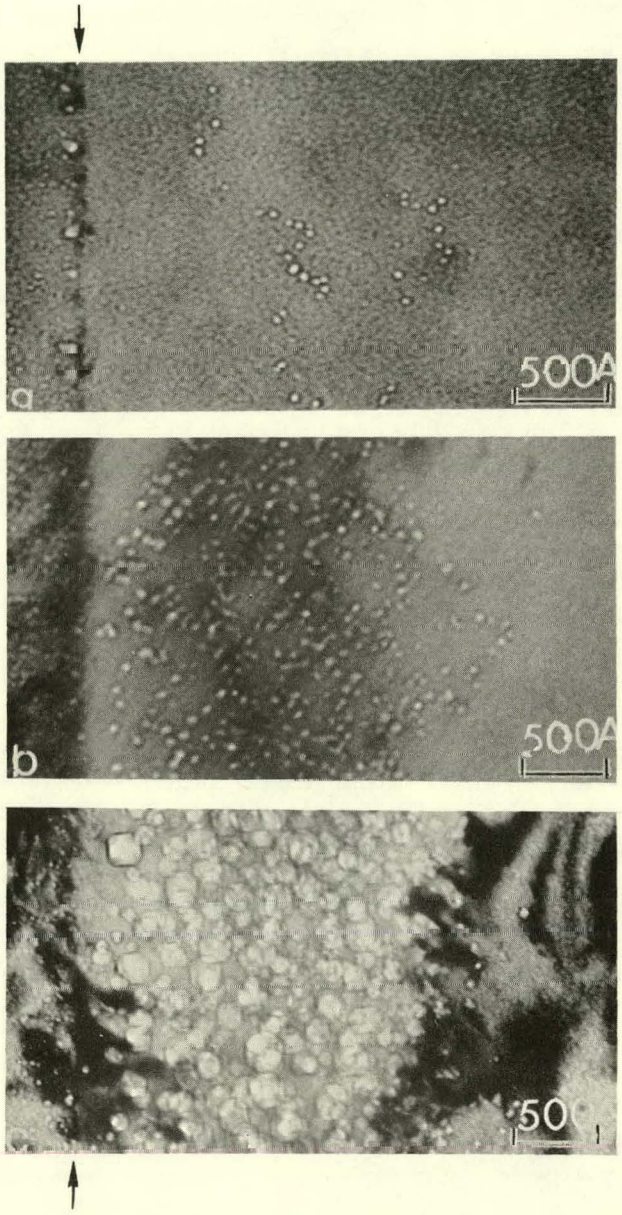

Figure I-1. Transmission electron micrographs of annealed polycrystalline nickel irradiated at 500°C with 20-keV $^4He^+$ ions for total doses of (a) 2.9×10^{15} ions/cm^2, (b) 2.9×10^{16} ions/cm^2, and (c) 2.9×10^{17} ions/cm^2.

nickel irradiated at 500°C with 20-keV $^4He^+$ ions to total doses of 2.9×10^{15}, 2.9×10^{16} and 2.9×10^{17} ions/cm^2, respectively. The interface between the plating and the irradiated region is marked by the vertical arrows. It can be seen in Figure I-1 that with increasing dose, both the size and the number density of cavities (bubbles or voids) increase. Quantitative measurements of diameter and number density of the cavities were made from high magnification micrographs for depth intervals of 250 Å from the surface, taking into account the measured variation in foil thickness. The average cavity diameter for a dose of 2.9×10^{15} ions/cm^2 ranged from 34-62 Å and it increased to 48-150 Å for a dose of 2.9×10^{17} ions/cm^2. The maximum value of the number density of the cavities increased from 3.4×10^{16} to 1.8×10^{17}/cm^3 as the total dose was increased from 2.9×10^{15} to 2.9×10^{16} ions/cm^2. Estimates of the volume fraction of cavities, $\Delta V/V$ as a function of depth (as measured from the irradiated surface) for total doses of 2.9×10^{15}, 2.9×10^{16} and 2.9×10^{17} ions/cm^2 indicate that the peak in the swelling occurs at a much larger depth (by almost a factor of 2) than the peak in the calculated projected range distribution. However, the depth at which the swelling peak occurs agrees very well with the mean blister skin thickness of ~ 0.15 μm. These results suggest that the separation of blister skin occurs at a depth where the volume fraction of the helium bubbles is at a maximum.

2. Surface Damage of Al Irradiated with $^4He^+$ to High Doses

M. Kaminsky and S. K. Das, Physics Division

Previous studies[6] of the surface damage of Nb after $^4He^+$ ion irradiation to high doses ($\sim 1.2 \times 10^{20}$ ions/cm^2) have been extended to annealed polycrystalline Al. The Al targets were irradiated with 20-keV and 100-keV $^4He^+$ ions to a dose of 1.2×10^{20} ions/cm^2, and the target temperatures were held at room temperature and at 250°C, respectively, for the two energies used. Figure I-2 shows SEM micrographs of an Al surface after it had been irradiated with 20-keV $^4He^+$ ions to four different dose values: 4.6×10^{18} ions/cm^2, 6.2×10^{18} ions/cm^2, 3.1×10^{19} ions/cm^2 and 1.2×10^{20} ions/cm^2. For the lowest dose one observes that in many surface areas as many as 12 layers (each layer corresponding to one blister skin thickness) have been lost. For the next larger dose, areas with a loss of 15 layers can be observed. For a dose of 3.1×10^{19} ions/cm^2 the surface appears very spongy and large cracks can be observed. For the largest dose of 1.2×10^{20} ions/cm^2, many large protrusions can be observed on a very spongy surface. Figure I-3 shows SEM micrographs of an annealed Al surface after it had been irradiated with 100-keV $^4He^+$ ions to a dose of 1.2×10^{20} ions/cm^2 at 250°C. One can readily see that in many areas, 12 layers (each layer with a "skin thickness" of ~ 0.6 μm) have been lost. These results on Al surfaces irradiated with $^4He^+$ ions to high doses indicate that no equilibrium surface structure has been reached, an observation we had already reported earlier for Nb.[6] It may be of interest to note that for similar irradiation conditions (100 keV $^4He^+$, 1.2×10^{20} ions/cm^2, homologous temperature range 0.3-0.4 T_m) significantly more layers were lost in the Al sample (~ 3 more layers). Based on the estimates of flux of 100-keV He^+ to the first wall in UWMAK-I, the high dose of 1.2×10^{20} ions/cm^2 corresponds to a period of 22 years of continuous operation. Thus, during the first 20-year lifetime of a first wall

---

6 M. Kaminsky, Proceedings of VII International Conference on Atomic Collisions in Solids, Moscow, USSR, September 18-23, 1977.

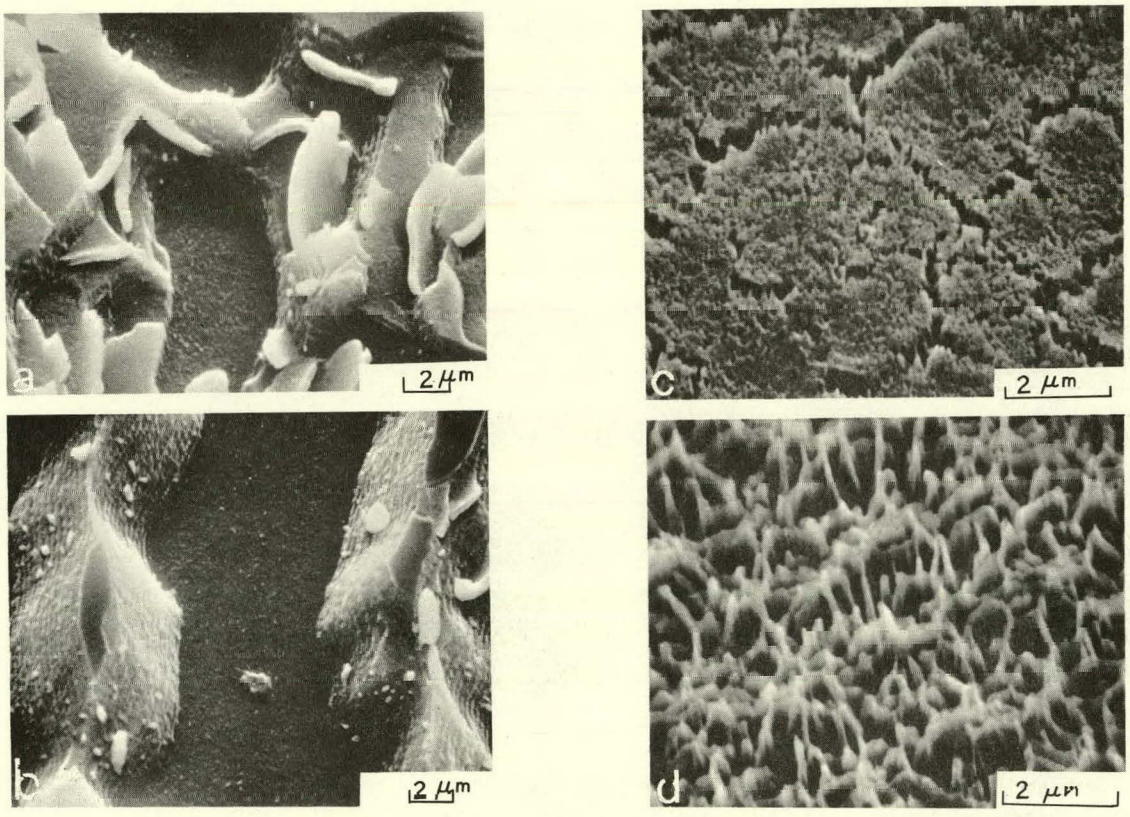

Figure 1-2. Scanning electron micrographs of annealed polycrystalline aluminum irradiated at room temperature with 20-keV $^4He^+$ to total doses of (a) 4.6×10^{18} ions/cm^2 (b) 6.2×10^{18} ions/cm^2, (c) 3.1×10^{19} ions/cm^2, and (d) 1.2×10^{20} ions/cm^2.

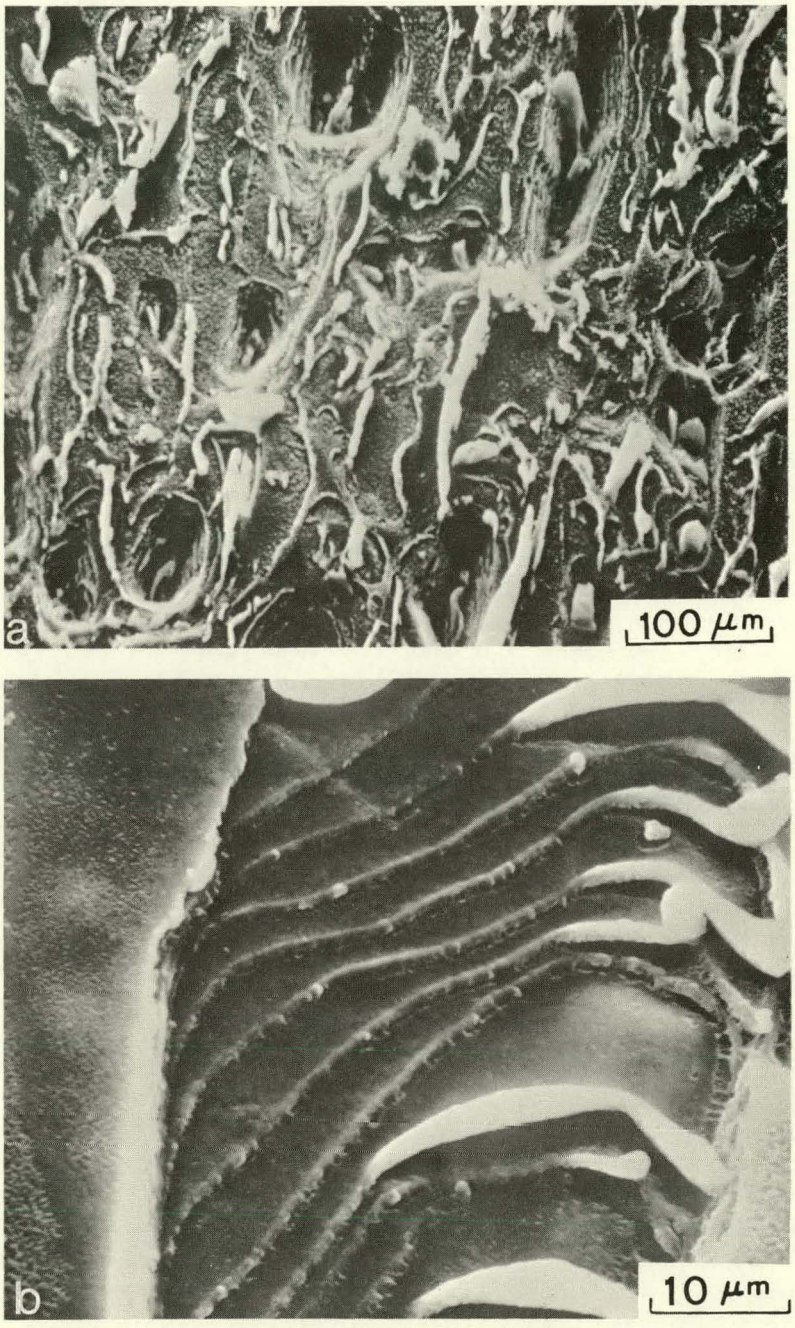

Figure I-3. (a) Scanning electron micrographs of annealed polycrystalline aluminum irradiated at 250°C with 100-keV $^4He^+$ to a total dose of 1.2×10^{20} ions/cm^2. Figure I-3(b) is an enlarged view of an area in Figure I-3(a) showing multiple exfoliation of blister skins.

of a fusion reactor, surface erosion due to blister skin exfoliation may play an important role and cannot be neglected as has been suggested by R. Behrisch, et al.,[7] and B. Scherzer.[8]

---

[7] R. Behrisch, et al., Proceedings of the 9th Symposium on Fusion Technology Pergamon Press, New York 1976, p. 531.

[8] B. M. U. Scherzer, J. Vac. Sci. & Tech. 13, 420 (1976).

3. Secondary Photon Emission from Ion Bombarded Surfaces

D. M. Gruen and R. B. Wright, Chemistry Division

A study of ion bombarded beryllium and graphite using secondary photon emission was undertaken during this period and will be briefly described. The experimental equipment used in this study and some preliminary results have been previously described.[9]

The present study investigated the effects of the incident ion beam energy and current density on the secondary photon emission of Be. Ion beams of Kr^+, Ar^+, Ne^+, He^+, O_2^+, N_2^+, D^+, D_2^+, H^+ and H_2^+ were used over the energy range of 300 eV - 15 keV. Ion beam current densities varied from a few tens to several hundred $\mu amp/cm^2$. Polycrystalline Be was used; the incident ion beam was perpendicular to the target surface, the emission observed at right angles to the ion beam. It was found that a prolonged (several days) sputter cleaning of the Be surface with 3 keV Ar^+ at 24 μamp current was required before the sample surface was sufficiently "clean". "Clean" in this context refers to signal stability (intensity) with time, which would continuously decrease until an equilibrium value, dependent on the residual gases present in the target chamber, was reached. Independent Auger analysis indicates that the "dirty" surface is mainly an oxide layer which must be removed in situ in the target vacuum chamber, the partial pressures of O_2 and H_2O being kept as low as possible. The "cleaned" surface would oxidize over a period of time once the ion beam was shut off, even though the sample was maintained under vacuum. The peak intensity of four atomic Be(I) (2348.6 Å, 2494.7 Å, 2650.6 Å and 3321.1 Å) and one ionic Be(II) (3130.7 Å) electronic emission lines arising from excited Be atoms and ions created during the sputtering process were monitored as functions of ion beam energy and current density. The incident beams of O_2^+, N_2^+, D_2^+ and H_2^+ were treated as being equivalent to O^+, N^+, D^+ and H^+ beams of half the energy and twice the current density. Results for one atomic line (Be(I) - 2348.6 Å) are shown in Figure I-4 as a function of incident ion energy and incident ion. It is observed that the intensity decreases in a non-linear manner as the incident beam energy is decreased. The intensity approaches zero before the beam energy does, a result expected due to the threshold energy required for sputtering. Furthermore, there is a great variation in intensity between the various incident beams, the current density remaining constant. Comparing the intensities, for example, at one energy (≈ 1000 eV) the relative values are for He^+:

---

[9] W. M. Stacey, Jr., et al., Fusion Power Program Quarterly Progress Report, January-March, 1977, Argonne National Laboratory, ANL/FPP-77-1 (1977).

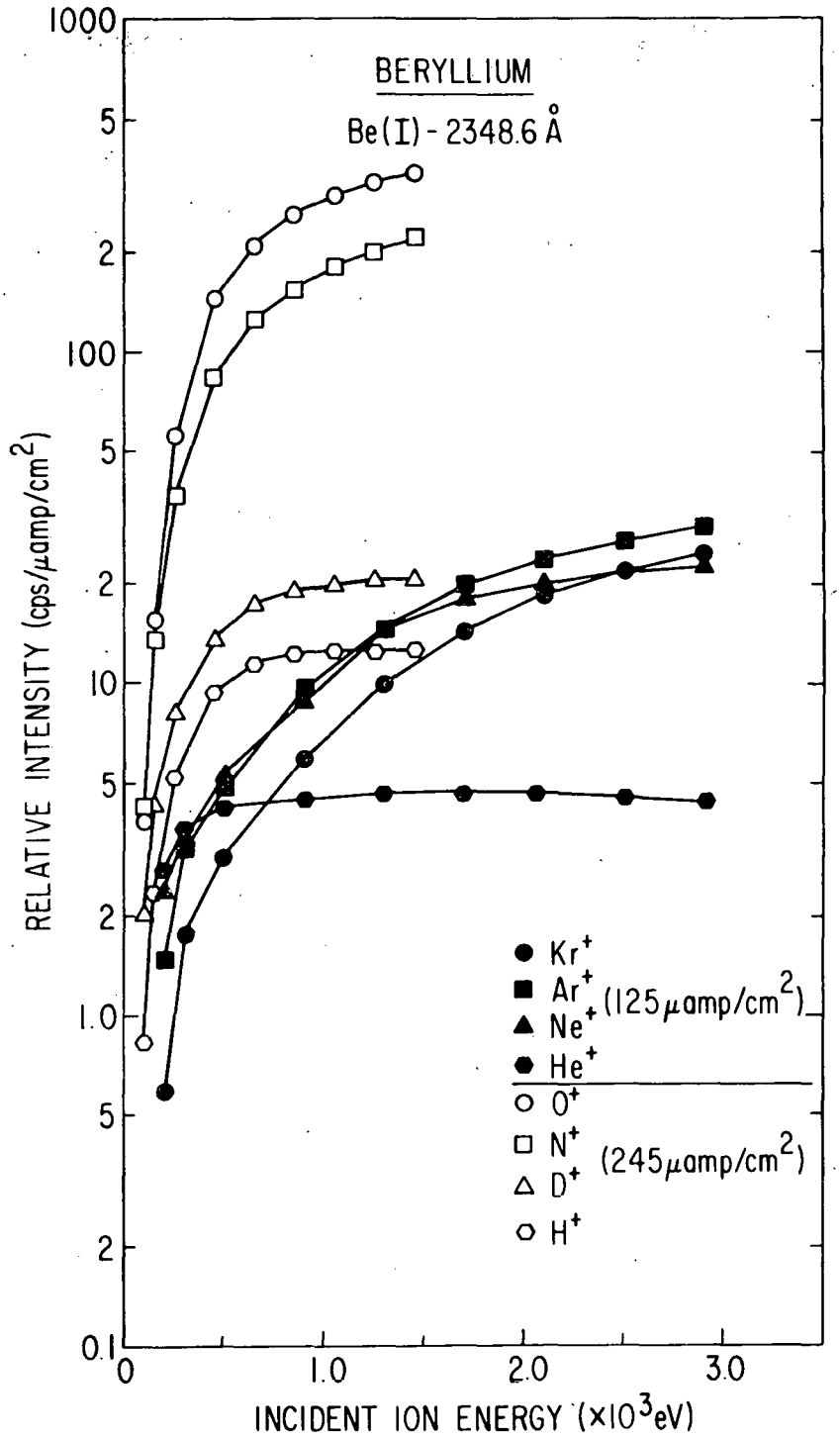

Figure I-4. Secondary photon emission intensity of Be(I) - 2348.6 Å line from a "clean" beryllium surface as a function of incident ion energy for various incident ions.

Ne^+: Ar^+: Kr^+: H^+: D^+: N^+: O^+ approximately 1:2:2.1:1.3:2.9:4.4:40.3:66.2, the ratios changing with beam energy. The intensity enhancement when the reactive beams are used (O^+, N^+, D^+, H^+) is surprising in that consideration of physical sputtering yields would predict $Kr^+ > Ar^+ > Ne^+ > O^+ > N^+ > He^+ > D^+ > H^+$. The other Be emission lines studies also displayed similar anomalous behavior. It should also be noted that the emission intensity due to excited Be^+ decreased faster with decreasing incident ion energy as compared with the excited neutral emission. The intensity of the same Be(I) line as a function of incident beam current density is shown in Figures I-5 and I-6. If the emission intensity were proportional to the current density, i.e., $I/J \alpha$ Const (I = intensity, J = current density) then the data should fall on a straight line of zero slope. This is seen not to be the case for all of the different incident ions. The intensity for the reactive O^+ and N^+ beams actually decrease in a non-linear manner with increasing current density (Figure I-6) whereas the intensity increases as $I \alpha J^{1.7}$ for the D^+ and H^+ beams. The inert gas beams also vary with current density except for He^+, which remains fairly constant. Similar behavior was exhibited by the other emission lines studied.

The observed intensity enhancement of the reactive gases O_2, N_2, D_2 and H_2 can partially be explained on the basis that non-radiative de-excitation of the excited states are reduced or prevented by the surface chemical changes induced by the reactive gas beams. The observed variation with inert gas beams cannot, however, be explained in this manner. That the chemical nature of the beryllium surface is altered by reactive beam bombardment was further supported by the following experiments. The beryllium surface was "cleaned" with an inert gas beam, then bombarded by a reactive gas beam, and subsequently re-bombarded by the inert gas beam. Significant intensity enhancements occurred with all the reactive gas beams which continuously decreased until the surface was sputter re-"cleaned" by the inert gas beam. The final equilibrium intensity corresponded to that for the initial "cleaned" state, prior to reactive beam bombardment. Upon exposure of the "clean" surface with the reactive gases (inert gas beam off) also initially enhanced the emission intensity, but the re-"cleaning" period when the inert beam was turned back on was substantially shorter (especially for N_2 and H_2 (or D_2) exposure) than it was when the reactive gas bombardment was used.

Excited molecular emission was also observed to occur from BeH and BeO. The BeH emission was always present but was enhanced during or after H^+ bombardment. BeO was observed during or after O^+ bombardment or after exposure to O_2 gas.

Two very weak lines were observed upon 15 keV Ar^+ bombardment of graphite (C(I) lines at 2479 Å and at 1931 Å). The low intensity prevented an analogous study of the beam energy and current density dependence from being performed. Also observed in the emission spectrum was the emission from excited molecular C_2.

The major conclusions of this research indicate that the observed phenomena arise from:

1. excitation: inelastic scattering processes occurring during the collision cascade are responsible for the creation of the excited

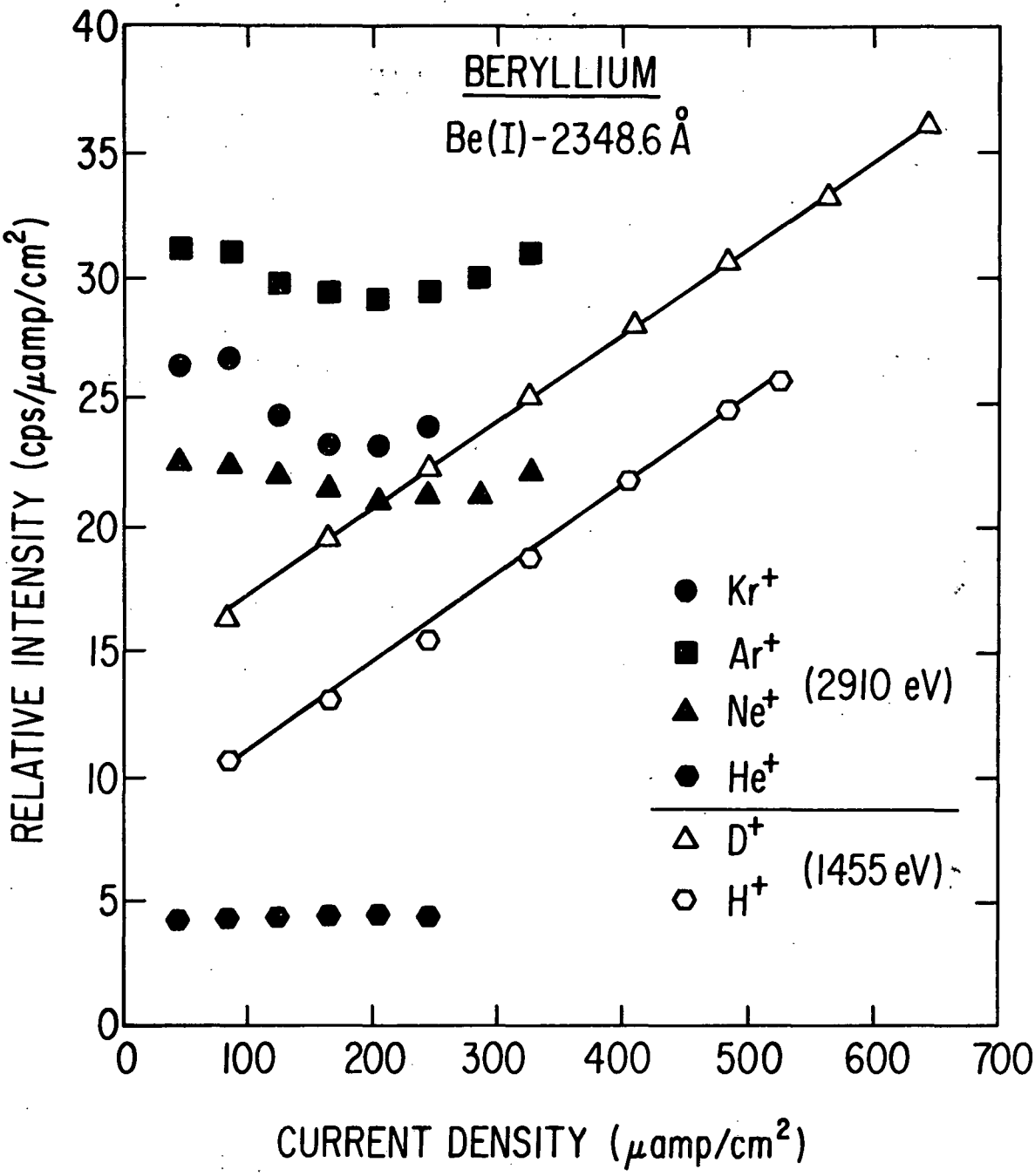

Figure I-5. Secondary photon emission intensity of the Be(I) - 2348.6 Å line from a "clean" beryllium surface as a function of incident ion current density (constant energy) for Kr^+, Ar^+, Ne^+, He^+, $D^+(D_2^+)$ and $H^+(H_2^+)$.

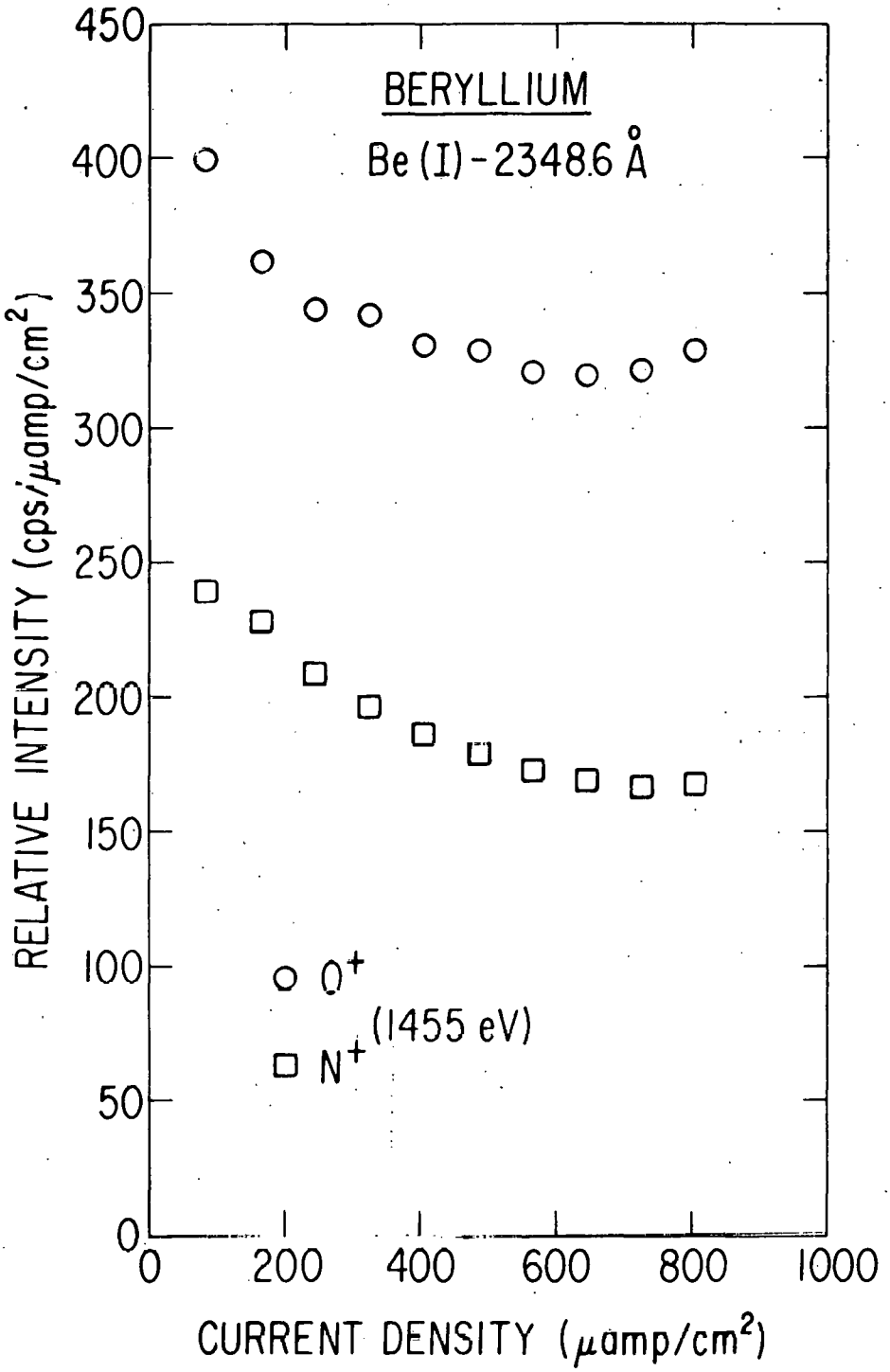

Figure I-6. Secondary photon emission intensity of the Be(I) - 2348.6 Å line from a "clean" beryllium surface as a function of incident ion current density (constant energy) for $O^+(O_2^+)$ and $N^+(N_2^+)$.

or ionic species and depend on the mass, energy (velocity) and electronic structure of the colliding pairs.

2. liberation: once excited the species must be removed from the surface for subsequent detection, therefore the sputtering mechanism and yield are intimately involved.

3. survival: once excited and sputtered, non-radiative de-excitation processes occuring at the surface-vacuum interface govern the number of excited sputtered neutrals or ions which survive to radiatively decay in vacuum. The chemical nature of the surface undergoing ion bombardment is a major influence governing their probability with respect to radiative de-excitation.

B. Dosimetry and Damage Analysis Work in Support of the MFE Materials Program

L. R. Greenwood and R. R. Heinrich, Chemical Engineering Division

1. Neutron Dosimetry

a. Experiments at the Oak Ridge Reactor (ORR)

The Oak Ridge Reactor (ORR) has been designated as a primary DMFE irradiation facility. Consequently, we have undertaken a major new effort to characterize the neutron environment. Three year-long irradiations, designated ORR-MFE-I through ORR-MFE-3, are planned for starts in February, June, and October of 1978, respectively. E. E. Bloom (ORNL) will coordinate the program which includes ANL, HEDL, ORNL, and NRL. We are responsible for dosimetry and damage analysis for each irradiation.

ORR-MFE-1, now being loaded in the reactor, will contain heaters to keep samples at temperatures up to 550°C. We placed four dosimetry wires, 24" in length, in each of the four quadrants of the irradiation assembly. The materials and expected reactions are listed in Table I-1. In one quadrant we also loaded 107 helium accumulation fluence monitors (HAFM) prepared by H. Farrar IV (Atomics International). This will allow us to directly compare our He gas rate calculations with experiment for Be, Al, K, Si, Ti, Fe, Cu, Ni, and Pb.

Since we have not studied ORR previously and since the reactor has a mixed thermal/fast spectrum, we have also planned a low power (~ 3 MW) spectral map to take place for about one day in late March 1978. This will allow us to study reactions with short half-lives, to use Cd covers to reduce the thermal flux on selected samples, and to use fission monitors with high heat generation rates. Two 24" long aluminum capsules were fabricated in the shops. One contained five spectral dosimetry sets and the other contained three sets, as listed in Table I-2. The sets were separated by aluminum spacers. The capsule with five sets also contained 26 HAFM materials from Al including ^{10}B, ^{6}Li, Al, B, Li, and Ni. The capsules were leak checked and welded. Four sets of wires, as listed in Table I-3, will also be used. This low power spectral run will be conducted in the same reactor location as ORR-MFE-2 and the samples will be returned to ANL as soon as possible following irradiation to facilitate counting.

Table I-1. Dosimetry Reactions for MFE Irradiations Fluence Monitor Gradient Wires in 6061 Aluminum Tube

Wire	Reaction	$t^{1/2}$
Fe (10 mil)	$^{54}Fe(n,p)^{54}Mn$	312.5 D
	$^{54}Fe(n,\alpha)^{51}Cr$	27.7 D
	$^{58}Fe(n,\gamma)^{59}Fe$	44.7 D
Co-Al (20 mil)*	$^{59}Co(n,\gamma)^{60}Co$	5.27 Y
	$^{59}Co(n,p)^{59}Fe$	44.7 D
	$^{59}Co(n,2n)^{58}Co$	70.85 D
Ni (10 mil)	$^{58}Ni(n,p)^{58}Co$	70.85 D
	$^{60}Ni(n,p)^{60}Co$	5.27 Y
Ti (10 mil)	$^{46}Ti(n,p)^{46}Sc$	88.9 D
	$^{47}Ti(n,p)^{47}Sc$	3.4 D
	$^{48}Ti(n,p)^{48}Sc$	1.8 D

* NBS alloy, 0.116 wt. % cobalt

b. Experiments at the University of California, Davis, Cyclotron - $^{9}Be(d,n)$ at E_d = 30 MeV

Dosimetry was provided for D. Styris (PNL) during May 1977 for the irradiation of tensile specimens (wires). Samples were placed immediately behind the beryllium target at an average distance of 4 mm from the source. Our dosimetry package was placed immediately behind the samples and consisted of 2" long by 1/4" wide strips of Al, Fe, Ni, Co, Nb, In, and Au giving us thirteen independent reactions to monitor for spectral unfolding. Short-lived activities were counted at Lawrence Livermore Laboratory and the others were counted by us. The dosimetry strips were cut into ten subsections in order to map flux and spectral gradients. The results for the four center cuts in the location of the tensile specimens are given in Table I-3. A complete activity map for $^{93}Nb(n,2n)^{92m}Nb$ is shown in Figure I-7. (The highest four center points correspond to Table I-3.) As can be seen, the gradients are very steep making accurate positional dosimetry a necessity. A complete error analysis is now in progress.

Two additional irradiations were conducted at E_d = 40 MeV in late February 1978 and similar dosimetry strips have been received for analysis.

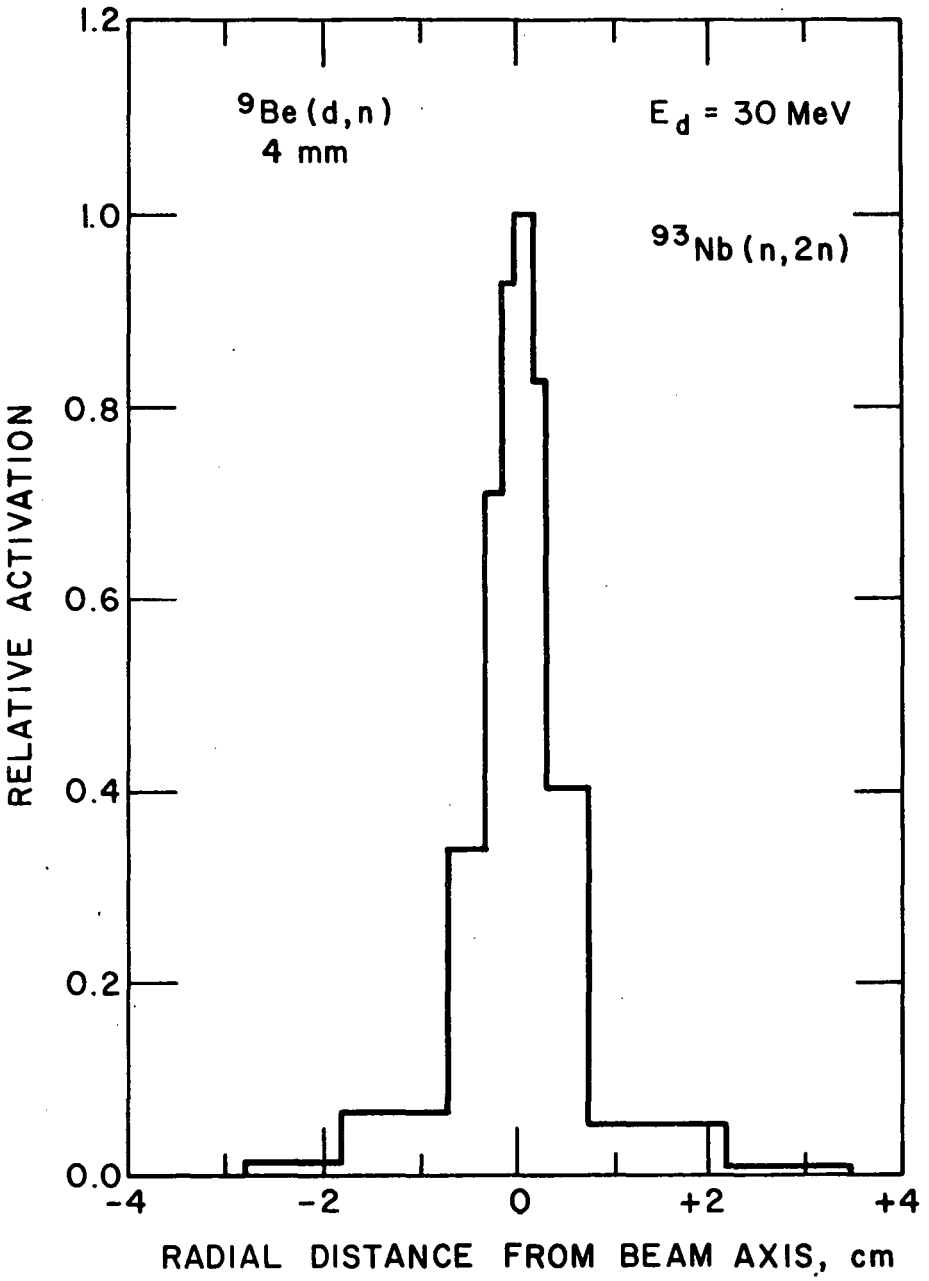

Figure I-7. Positional dosimetry results for D. Styris (PNL).

Table I-2. Dosimetry Reactions for ORR Spectral Mapping Wires and Foils in 6061 Aluminum Capsule

Material	Reaction	$t^{1/2}$	Cd Cover
$^{237}Np(n,f)$*	^{95}Zr	64.1 D	Yes
$^{235}U(n,f)$*	^{103}Ru	39.4 D	Yes
	^{131}I	8.0 D	
$^{238}U(n,f)$*	^{140}Ba	12.8 D	
^{238}U	$(n,2n)^{237}U$	6.75 D	
	$(n,\gamma)^{239}Np$	2.36 D	Yes
Ni (wire)	$^{58}Ni(n,p)^{58}Co$	70.85 D	
	$(n,2n)^{57}Ni$	36 H	
Co (wire)	$^{59}Co(n,\gamma)^{60}Co$	5.27 Y	Yes
	$(n,p)^{59}Fe$	44.6 D	
	$(n,2n)^{58}Co$	70.85 D	
Fe (wire)	$^{54}Fe(n,p)^{54}Mn$	312.5 D	
	$(n,\alpha)^{51}Cr$	27.7 D	
	$^{58}Fe(n,\gamma)^{59}Fe$	44.6 D	
Au	$^{197}Au(n,\gamma)^{198}Au$	2.7 D	Yes
	$(n,2n)^{196}Au$	6.1 D	
Ti	$^{46}Ti(n,p)^{46}Sc$	83.9 D	
	$^{47}Ti(n,p)^{47}Sc$	3.4 D	
	$^{48}Ti(n,p)^{48}Sc$	1.8 D	
Sc*	$^{45}Sc(n,\gamma)^{46}Sc$	83.9 D	Yes
	$(n,2n)^{44m}Sc$	2.44 D	

* In ORNL vanadium capsules

Table I-3. Flux Measurements for Styris 2 (PNL)

$^{9}Be(d,n)$ - E_d = 30 MeV

4 mm from source, current = 23.8 μA

Neutron Flux (x 10^{12} n/-cm^2-s)

Sample Width (mm):	1.2	1.5	1.8	0.9
Angular Range*:	-40° -28°	-28° -8°	-8° +17°	+17° +28°
Total flux	5.87	6.54	7.05	6.33
> 0.1 MeV	5.82	6.48	6.99	6.26
> 1 MeV	5.35	6.01	6.45	5.77
> 4 MeV	3.93	4.62	4.88	4.43
>10 MeV	2.33	2.83	3.06	2.70
>14 MeV	1.73	1.87	1.94	1.71

* Estimated; + and - refer to degrees above or below the beam axis, respectively.

2. Damage Analysis

L. R. Greenwood, Chemical Engineering Division

a. Error Analysis

We have now completed development of our error analysis capabilities for all damage parameters. The code SPECTRE has been modified to use the complete error covariance matrix generated by our Monte Carlo error analysis code SANDANL. Elements of the matrix are determined directly from the Monte Carlo variations by calculating cross-correlation coefficients. We can thus directly determine the errors in damage parameters caused by uncertainties in our neutron dosimetry. Sample output is shown in Table I-4 for the $^{9}Be(d,n)$ spectrum measured at the ANL Tandem Van de Graaf Accelerator at E_d = 16 MeV.

As can be seen, the errors are typically 5-10% and are much less than the errors in the differential spectrum due to the strong cross-correlations in the differential flux spectrum. We should note that errors in displacement cross sections themselves are not included so that the errors in Table I-4 are solely due to our dosimetry measurements.

Table I-4. Error Analysis for ANL Tandem Van de Graaf

$^{9}Be(d,n)$ E_d = 16 MeV

$\phi = 7.9 \pm 0.5 \times 10^{9}$ n/cm^2-s

Element	DPA[a] (10^{-11}/s)	<H>[b] (10^{-11} ppm/s)	<He>[b] (10^{-11} ppm/s)
Al	1.44 ± 0.11	30.2 ± 2.2	20.3 ± 1.5
Ni	1.24 ± 0.09	20.3 ± 1.6	40.1 ± 2.8
Nb	1.07 ± 0.08	7.56 ± 0.52	1.26 ± 0.09

PKA[c] Energy Range (keV)	Primary Knock-on Atoms (%) Al	Ni	Nb
1	1.2 ± 0.2	3.3 ± 0.5	5.5 ± 0.7
1 - 10	9.7 ± 1.4	20.1 ± 1.8	31.6 ± 5.2
10 - 40	22.9 ± 4.1	30.8 ± 2.5	30.0 ± 4.7
40 - 100	23.8 ± 3.3	20.3 ± 1.6	19.6 ± 1.4
100 - 300	23.4 ± 1.7	18.8 ± 1.1	12.3 ± 0.5
> 300	19.1 ± 0.9	6.7 ± 0.3	0.9 ± 0.04

[a] Displacements-per-atom

[b] Gas generation rates do not include secondary reactions such as (n,nα)

[c] Energy distribution of primary displacement atoms.

b. Dosimetry Analysis

The SAND II spectral unfolding code has been modified to include self-shielding and cadmium cover effects exactly. These corrections will be required at ORR and other mixed spectrum facilities where resonance effects predominate. For example, at least 50% of the activation of $^{197}Au(n,\gamma)$ ^{198}Au is due to a single narrow resonance at 4.9 eV which has a peak cross section near 40,000 barns! However, thick foils (e.g., ∿ 1 mil) will not

indicate this effect since the neutrons near the resonance energy will be totally absorbed near the surface of the foils and will not penetrate to the inside atoms. This effect is called self-shielding and must be allowed for with all resonance as well as high thermal detectors.

Unfortunately, self-shielding factors can not be determined unless one knows the spectrum which is being measured. This problem can be avoided by lumping the self-shielding and cadmium cover effects into the cross-sections used by SAND II. New self-shielding effects are then automatically included with each iteration.

We have written a code RESATN which corrects the SAND II cross section library for each case of self-shielding by making very detailed calculations over each narrow resonance for each material. The calculations are based on formula derived by K. M. Case, et al.[10] Wires and foils can be used with either a beam or isotopic flux geometry. End effects are also considered to first order by replacing the actual foil thickness or wire diameter by the mean chord given by $xyz/(xy + xz + yz)$ for a foil of length x, width y, and thickness z, or $2dl/(d + 2l)$ for a wire of diameter d and length l.

---

[10] K. M. Case, F. de Hoffman, G. Placzek, Introduction to the Theory of Neutron Diffusion, Los Alamos, (1953).

C. Alloy Development

1. Hydrogen Permeation and Materials Behavior in Alloys of Interest to the Fusion Power Program

Recent emphasis in this program has been directed towards (1) studies of hydrogen permeation in representative austenitic and nickel-base alloys and (2) construction of a small (∿ 0.5-liter capacity) stainless-steel-clad vanadium alloy lithium loop. Progress in these two areas during the first quarter of FY-1978 is summarized below.

a. Hydrogen Permeation Studies

E. H. Van Deventer and V. A. Maroni, Chemical Engineering Division

A series of studies is underway to determine the hydrogen permeation characteristics of selected austenitic and nickel-base alloys over a wide range of hydrogen driving pressures and temperatures. The principal objectives of these studies are to (1) determine the effects of various impurity and ionizing radiation environments on permeation rates, (2) search for departures from square-root of pressure dependence and evaluate their causes, and (3) expand and augment the permeation data base for alloys that have been employed as substrates in our barrier development work and that are of current interest to the fusion program in general. During the past quarter, studies of Inconel-625 and 316-SS have been completed.

Additional features incorporated into the permeation apparatus in recent months now permit us to monitor and control (to a considerable extent) gas compositions in the upstream compartment. For the measurements reported herein, continuous monitoring of the upstream gas composition (using a partial pressure analyzer) revealed that at low upstream hydrogen pressures, water, carbon monoxide/nitrogen,* argon, and helium can combine to make a significant contribution to the total pressure in the upstream compartment. In some cases,the molecular hydrogen partial pressure was found to constitute as little as 20% of the total pressure. It became evident from this observation that a total pressure measurement does not necessarily represent an accurate determination of the molecular hydrogen activity when the upstream pressure is relatively low (i.e., < 1 Pa). Best results in terms of achieving a high purity hydrogen environment were obtained using a temperature controlled uranium hydride bed (to regulate H_2 pressure) in combination with a throttled ion-pump. The presence of uranium hydride in the upstream system caused a substantial reduction in the active gases (e.g., H_2O, O_2, N_2/CO) while the throttled ion-pump helped to remove the inert gases (e.g., He, Ar). Many of the simulated environments used during the course of these experiments were considered to be representative of plasma chamber exhaust gas compositions for near-term fusion devices.

Permeation data for 316-SS and Inconel-625 as a function of temperature are shown in Figures I-8 and I-9, respectively. Least-squares refined permeation curves based on the data in Figures I-8 and I-9 may be represented by equations (1) and (2)

$$\phi_{316\text{-SS}} = 0.182 \exp(-15{,}175/RT) \quad (1)$$

$$\phi_{\text{Inconel-625}} = 0.198 \exp(-14{,}371/RT) \quad (2)$$

where ϕ is in units of $cm^3(STP)/m \cdot s \cdot kPa^{1/2}$, R is equal to 1.987, and T is in K. The data employed to derive equations 1 and 2 were collected under conditions where hydrogen averaged greater than 99% of the gas phase species present. Under these conditions, a near-to-half-power dependence on driving pressure was observed over the entire pressure range of the study. In cases where oxygen bearing species dominated the gas phase in the upstream compartment, measurable deviations towards a closer-to-first-power dependence on hydrogen pressure were observed at the lower end of the pressure range (i.e., 10^{-1} to 1 Pa). Also, no changes in permeation rate were observed for 316-SS when a 1 mCi γ-source was placed inside the upstream compartment in close proximity to the upstream surface of the sample. This result confirms that an ionizing radiation environment (e.g., as in the vicinity of a fusion reactor first wall) will not affect permeation rates that are controlled by bulk diffusion mechanisms.

---

* It is not possible to distinguish between N_2 and CO (both mass 28) with the partial pressure analyzer. Both are known to be present from other tests.

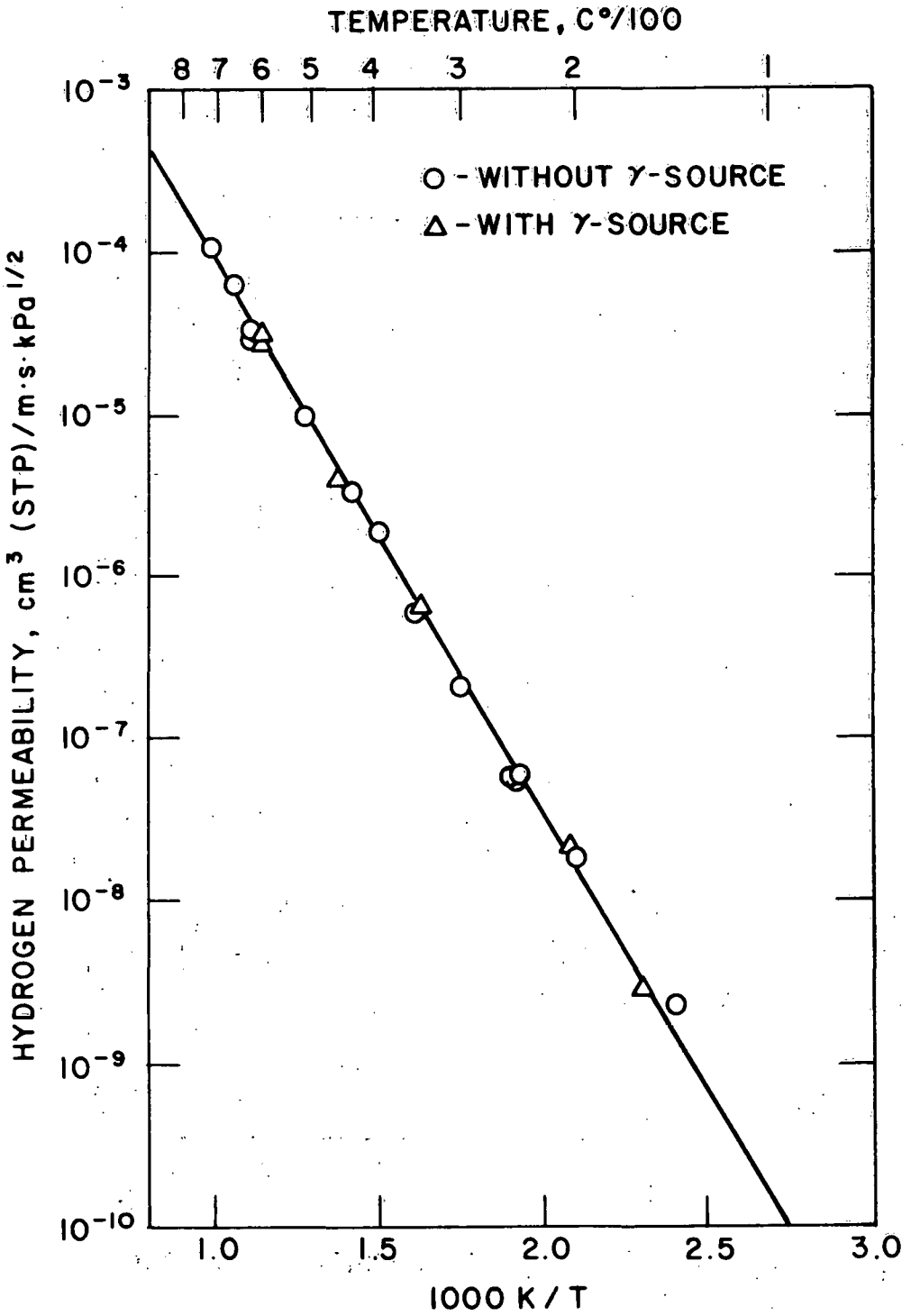

Figure I-8. Hydrogen permeation data for 316-SS.

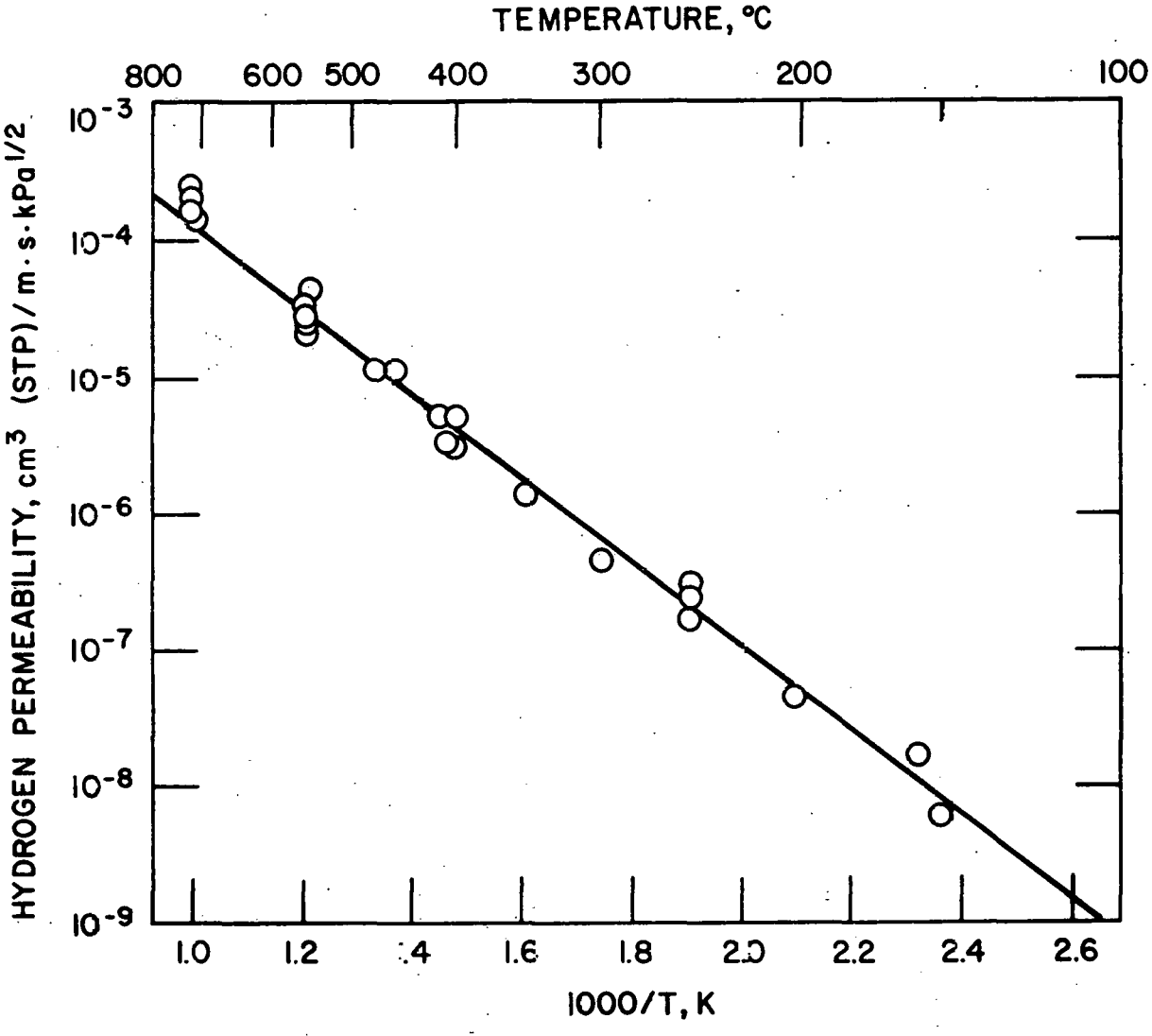

Figure I-9. Hydrogen permeation data for Inconel-625.

Plots of the relationship between permeation rate and hydrogen partial pressure in the upstream compartment obtained for 316-SS and Inconel-625 are given in Figures I-10 and I-11, respectively. The data presented in these figures were collected under conditions where hydrogen was the major species in both upstream and downstream gas phase environments. The small departures from an exact half-power dependence are probably due in part to experimental uncertainty and in part to factors attributable to impurity interactions with the surfaces of the permeation samples.

b. Tests of Vanadium Alloy Performance in a Liquid Lithium Environment

D. L. Smith, Materials Science Division, and V. A. Maroni, Chemical Engineering Division

The effort to assemble a small lithium loop (~ 0.5 liter capacity) using a stainless-steel-clad vanadium alloy (V-15Cr) is nearing completion. This loop will be operated in an EM-pumped mode and will be used as a test of vanadium-alloy weld integrity, cladding integrity, and materials performance in a circulating lithium environment. It is expected that this loop will be ready to run by the end of March. All phases of this project have been carried out by members of the ANL Materials Science Division.

c. Swelling Behavior of Dual-Ion Irradiated Fe-15Cr-20Ni Alloy: A Comparison of Preinjected Versus Simultaneously Injected Helium

S. C. Agarwal, D. I. Potter, A. Taylor, and F. V. Nolfi, Jr., Materials Science Division

An Fe-15Cr-20Ni austenitic alloy was irradiated simultaneously with He and Ni ions at the ANL Dual-ion Irradiation Facility to simulate the swelling behavior of this alloy in the presence of high transmutant helium production rates that will occur in structural materials in fusion reactors. Annealed specimens of this alloy were irradiated with a 3-MeV $^{58}Ni^{+}$ beam to produce displacement damage and simultaneously injected with He using a degraded 0.95-MeV $^{3}He^{+}$ beam. Nominal dose levels ranged from 3-25 dpa, the irradiation temperature was 700°C, and three nominal He:dpa (appm:dpa) ratios were used, viz., 5:1, 15:1, and 50:1. Specimens preinjected with 15 appm He and irradiated with only Ni^{+} ions under identical dose and temperature conditions were also included in this study for comparative purposes. In addition, a temperature dependence study was carried out in the range 600-800°C in order to determine any shift in the swelling peak associated with the high He levels. For this study, the dose and He:dpa ratio were held constant at 12 dpa and 15:1, respectively.

In the dose dependence study, a strong dependence of cavity microstructure on He:dpa ratio was observed. A bimodal size distribution of cavities was observed up to 6 dpa for the 15:1 He:dpa ratio and up to 25 dpa for the 50:1 He:dpa ratio. After 6 dpa (Figure I-12), the swelling increased rapidly for both the 15:1 and 50:1 He:dpa ratio specimens with the 50:1 specimens uniformly showing less swelling. This was associated with an increase in mean cavity diameter for both groups of specimens; the cavities in the 15:1

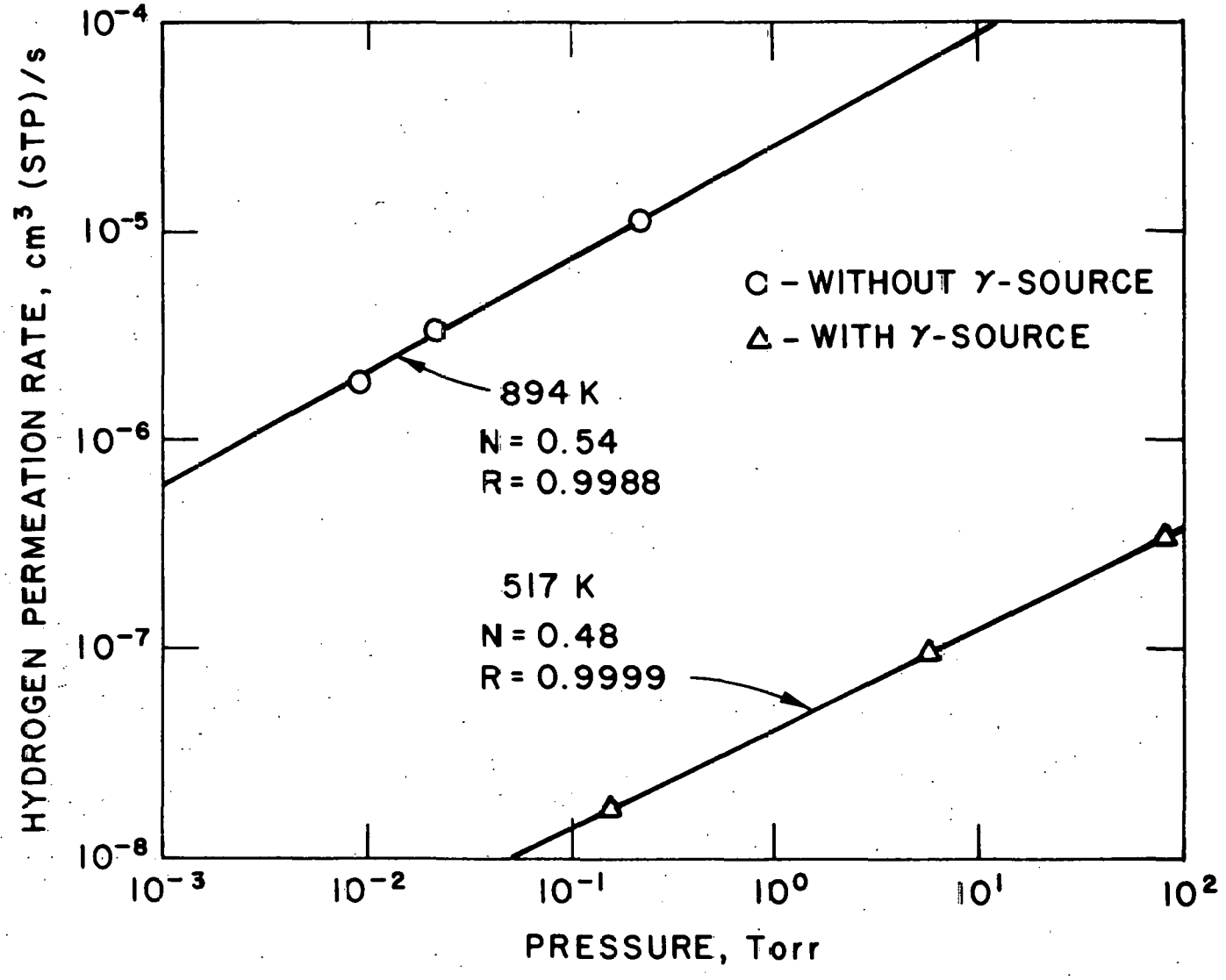

Figure I-10. Permeation rate versus hydrogen pressure for 316-SS. (N = Slope, R = Correlation Coefficient)

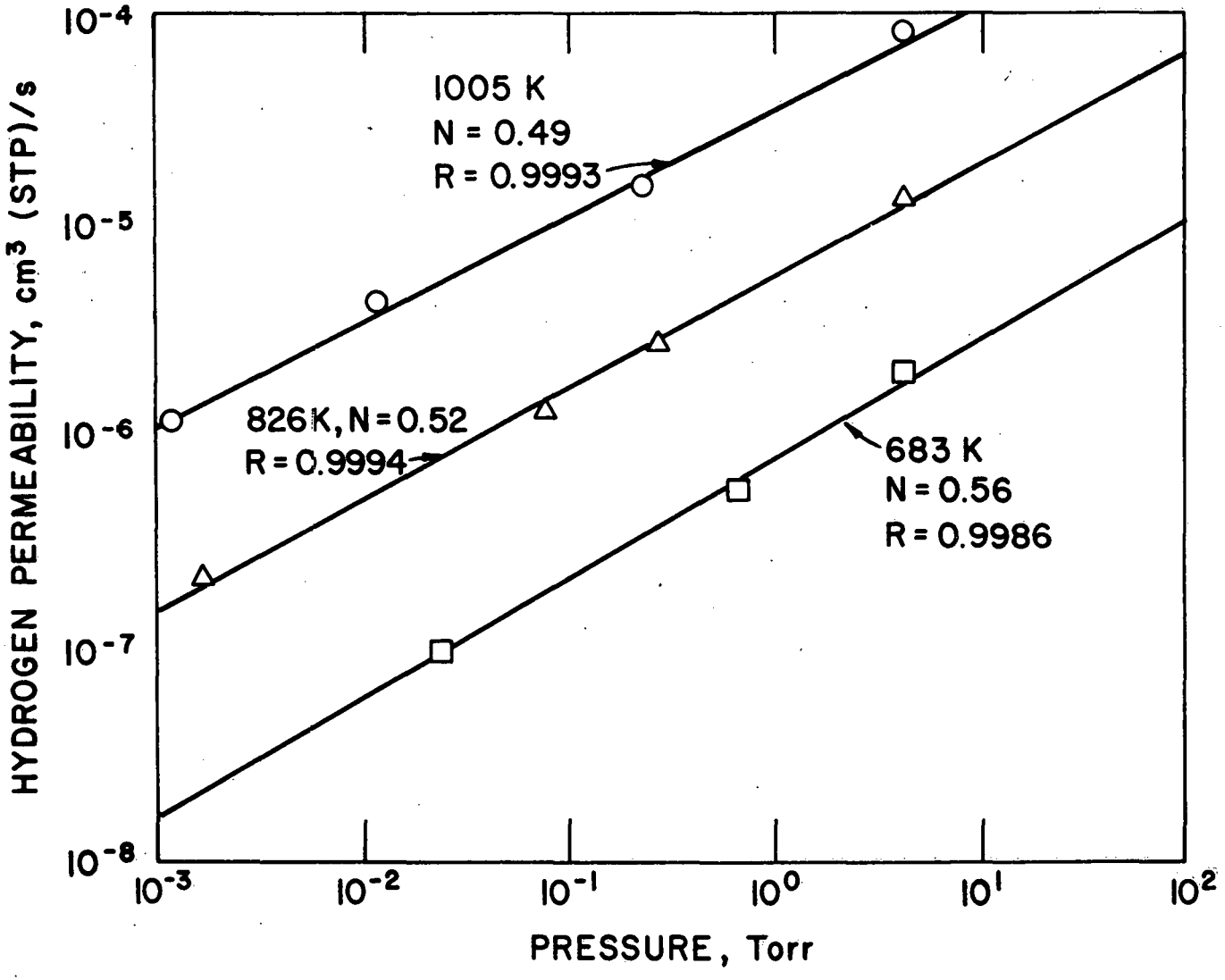

Figure I-11. Plot of permeation rate versus hydrogen partial pressure for Inconel-625. (N = Slope, R = Correlation Coefficient)

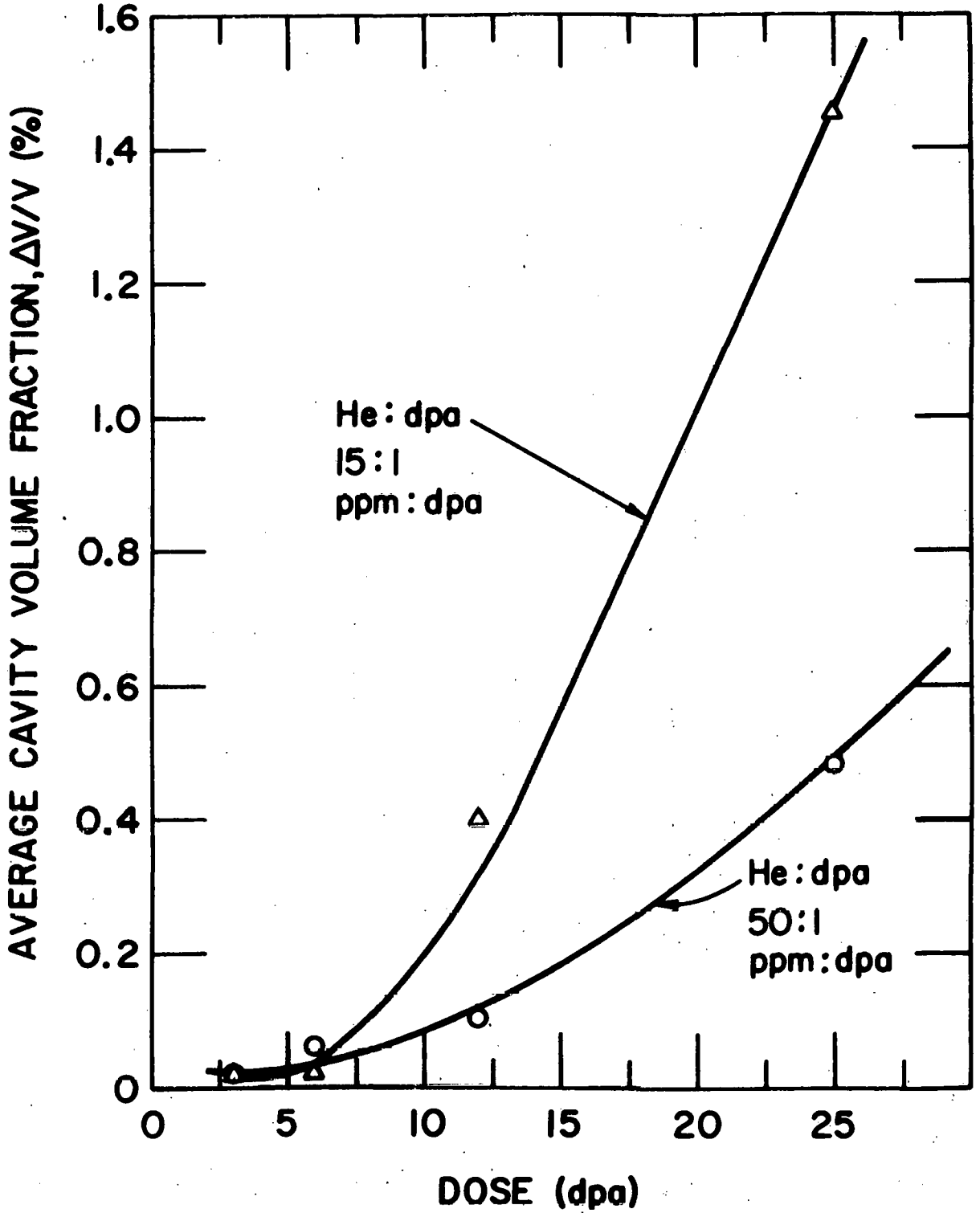

Figure I-12. Swelling vs dose curves for Fe-15Cr-20Ni alloy irradiated at 700°C.

specimens were larger and increased in size more rapidly than in the 50:1 specimens. For both He:dpa ratios, the cavity number densities decreased with increasing dose, and were observed to be generally higher for the 50:1 He:dpa ratio. These studies also showed that up to $\sim$ 6 dpa, the swelling is comparable for the two He:dpa ratios (15:1, 50:1) thus far examined.

From the temperature dependence study, peaks in both the swelling curve and cavity size were observed to occur at $\sim$ 650°C (Figure I-13). The cavity number density and dislocation density decreased with increasing temperature and showed a plateau in the vicinity of the swelling and cavity size peak.

The present results show that simultaneous He injection at the higher He:dpa ratio reduces swelling by inhibiting cavity growth. Furthermore, for a given He:dpa ratio and dose, an effect of simultaneous He injection is to inhibit cavity growth at higher temperature.

2. Radiation Damage of Diagnostic Windows in TFTR

W. Primak, Solid State Science Division

Calculations of radiation effects to be anticipated in a vitreous silica window were continued to include the effects from soft X-ray emission from tungsten impurities. The surface energy deposition was formidable, 30,000 cal/g per pulse, but the absorption was so great that by 0.1 μ below the surface it fell below 14,000 cal/g per pulse. The ionization density was sufficiently low to consider that the material would behave in a classical thermal manner with customary thermal constants. The temperature rise of the surface was estimated as 112°C. Heat transfer could probably be handled by suitable design because the duty cycle is so low, 1/2 second heating and 5 minute cooling. However, the radiation effects might be large enough to initiate crazing of the window. It was therefore recommended that the window be protected with a thin cover slip of the same material with a gap which would permit this cover slip to reach temperatures at which radiation effects anneal.

Calculations were also begun for a crystal quartz window. Experimental data corresponding to the conditions to be encountered do not exist and the data base from which the behavior could be estimated is much smaller than for vitreous silica. It was estimated that the behavior toward the neutron flux would be comparable to that estimated for the vitreous silica. Best current information would indicate that the ionization effects in quartz are less severe than in vitreous silica, but experimental information is not adequate to be certain of this. Information on the specification and selection of crystal quartz suitable for the application was supplied.

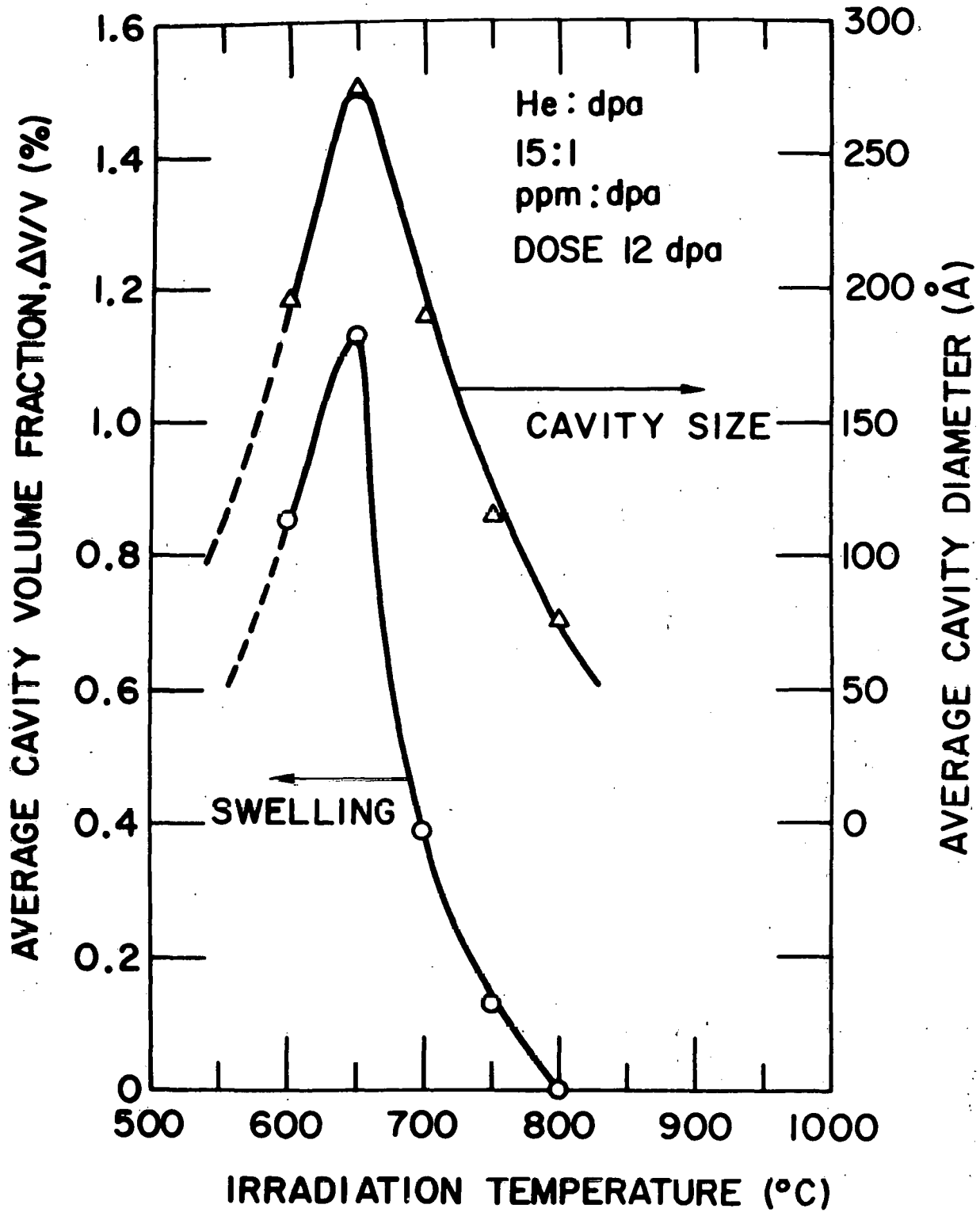

Figure I-13. Temperature dependence of swelling and cavity size in dual-ion irradiated Fe-15Cr-20Ni alloy.

D. Special Purpose Materials Development

1. Fast-Neutron Irradiations of Superconducting Nb_3Sn

B. S. Brown and T. H. Blewitt, Materials Science Division

The superconducting magnets that will be used for the plasma confinement in fusion reactors will be subjected to irradiation by neutrons penetrating the shield and blanket. Therefore, it is necessary to know the effect of the radiation on the properties of the various magnet components. The superconducting composite wire will contain NbTi for magnets with fields below 8 T, but for higher fields Nb_3Sn or another compound superconductor will be necessary. The effects of fast-neutron irradiation on the critical current of superconductors has been studied previously[11-13] and was discussed at the June, 1977 meeting on Radiation Effects on Superconductivity.[14]

The parameter of interest for the superconductors is the critical current density, (J_c), i.e. the maximum amount of current that the wire can carry without developing a voltage. J_c depends on the superconducting transition temperature and the defect microstructure, both of which are affected by fast-neutron irradiation. Since the fusion magnets will be irradiated while in the superconducting state, it is necessary that the design data be obtained from liquid-helium temperature irradiations. Also, previous investigations have shown that a wide variance in the critical-current changes (with dose) occurs, depending on the initial critical-current density, the irradiation temperature, and perhaps the neutron spectrum.[15] The four experiments reported here quantify these effects by irradiating high and moderate current density material at 6 K and 350 K (reactor ambient temperature) in the same neutron spectrum.

Figure I-14 shows the unirradiated values of J_c as a function of field H. The $J_c(H)$ for sample A is near the highest made for Nb_3Sn by the bronze diffusion technique. Figures I-15, I-16 and I-17 show the fractional changes in J_c (J_{co} = unirradiated value of J_c) as a function of field and dose for the different samples and irradiation temperature. The J_c for the moderate J_{co} samples (B) shows a very large enhancement with dose which is independent of irradiation temperature. The high J_{co} samples (A) show a much smaller enhancement than the B samples and the changes after the 6 K irradiation are more than twice those after the 350 K irradiation. These differences are explained in terms of the different magnetic flux pinning capabilities of the different defect structures that result during irradiations below and above the defect migration temperature.[16]

---

[11] B. S. Brown, et al., J. Appl. Phys. 46, 5163 (1975).

[12] M. Soell, et al., IEEE Trans. Mag. MAG-11, 178 (1975).

[13] B. S. Brown, et al., IEEE Trans. Mag. MAG-13, 659 (1977).

[14] Proc. Intl. Discussion Mtg. on Radiation Effects on Superconductivity, J. Nucl. Mater., in press.

[15] B. S. Brown, in Radiation Damage in Metals, eds. N. L. Peterson and S. D. Harkness, American Society for Metals, Metals Park, Ohio (1976).

[16] B. S. Brown, et al., J. Appl. Phys., to be published.

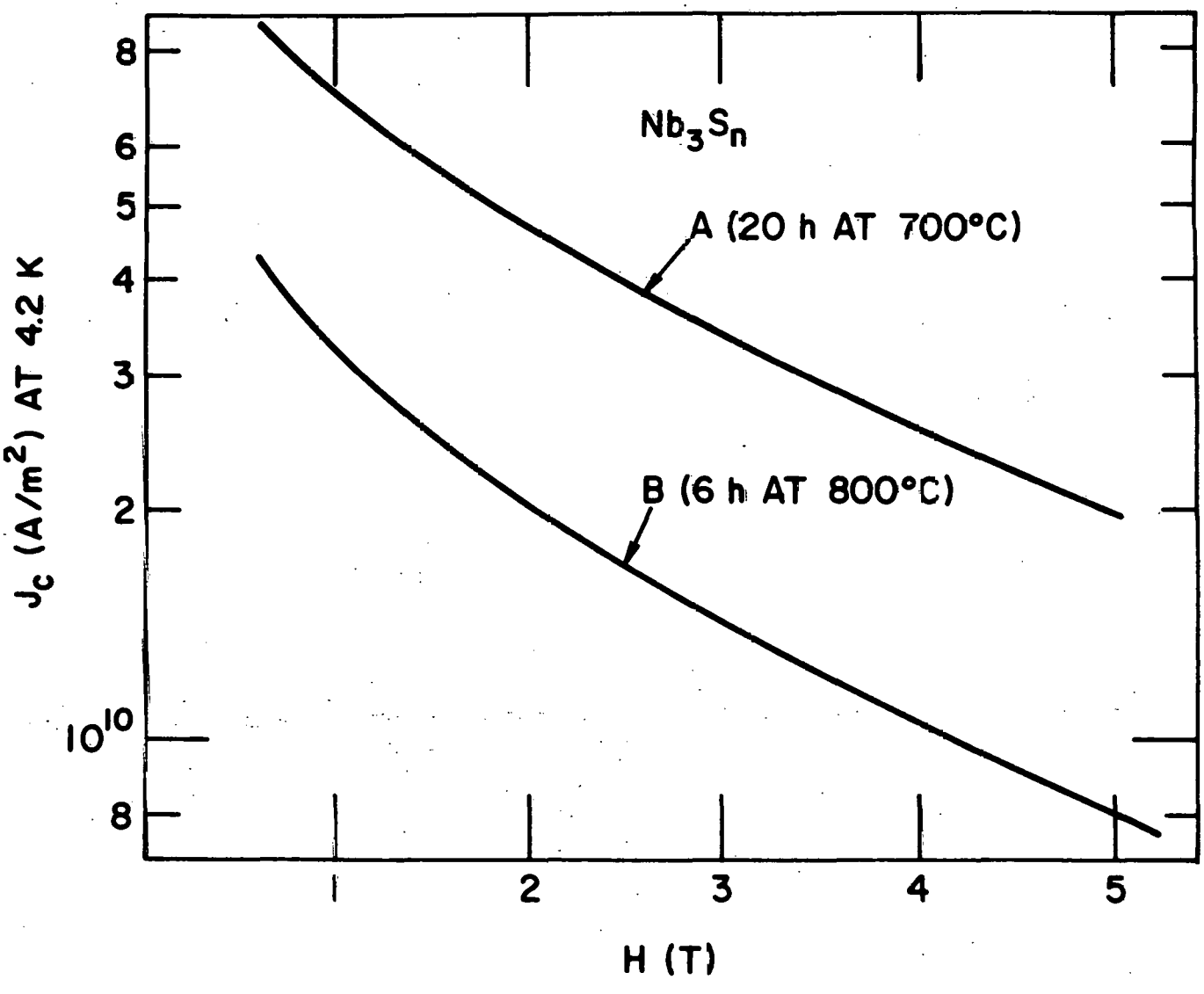

Figure I-14. Unirradiated critical-current density (J_{co}) as a function of applied field (H).

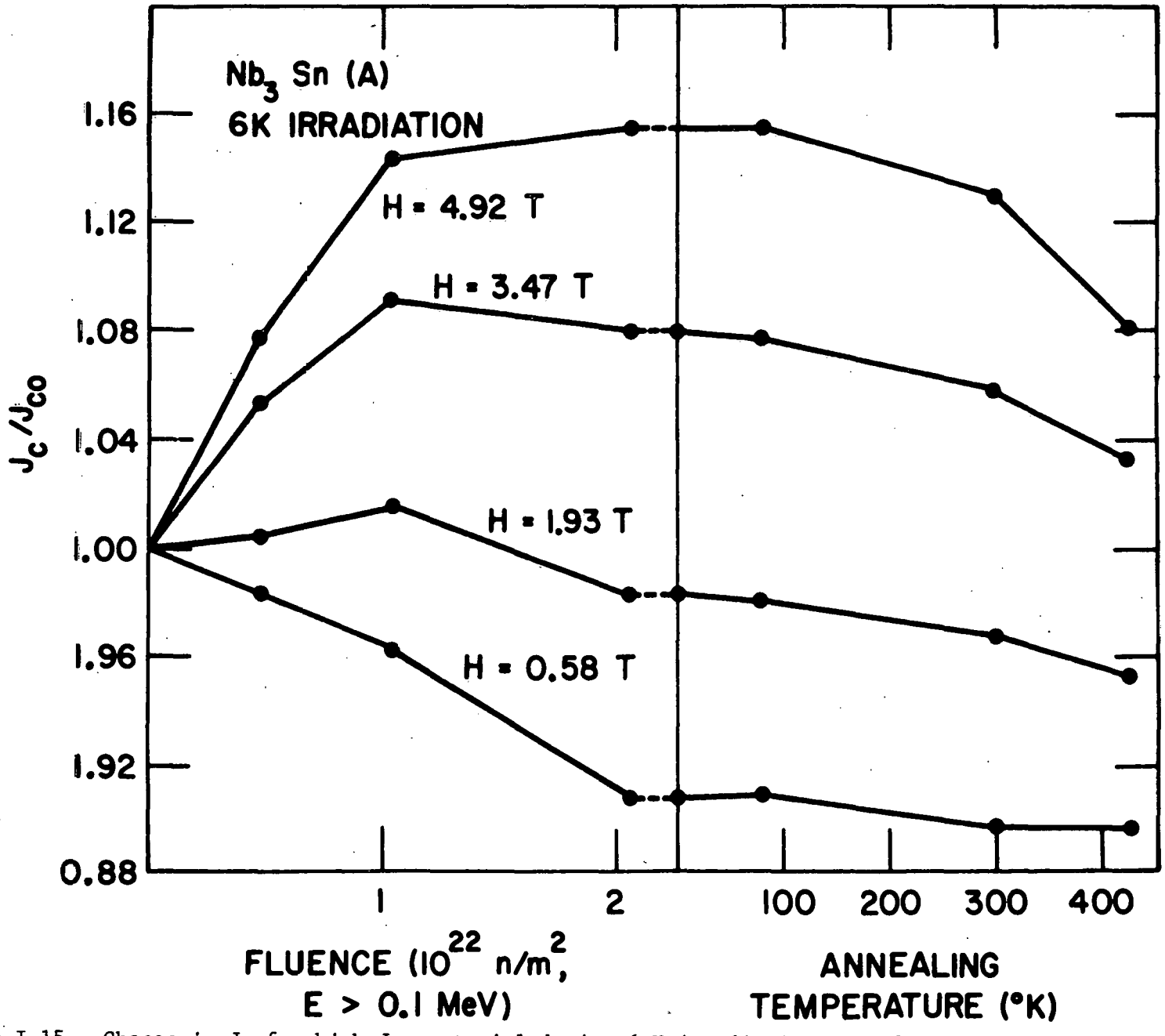

Figure I-15. Change in J_c for high J_{co} material during 6 K irradiation and after isochronal anneals.

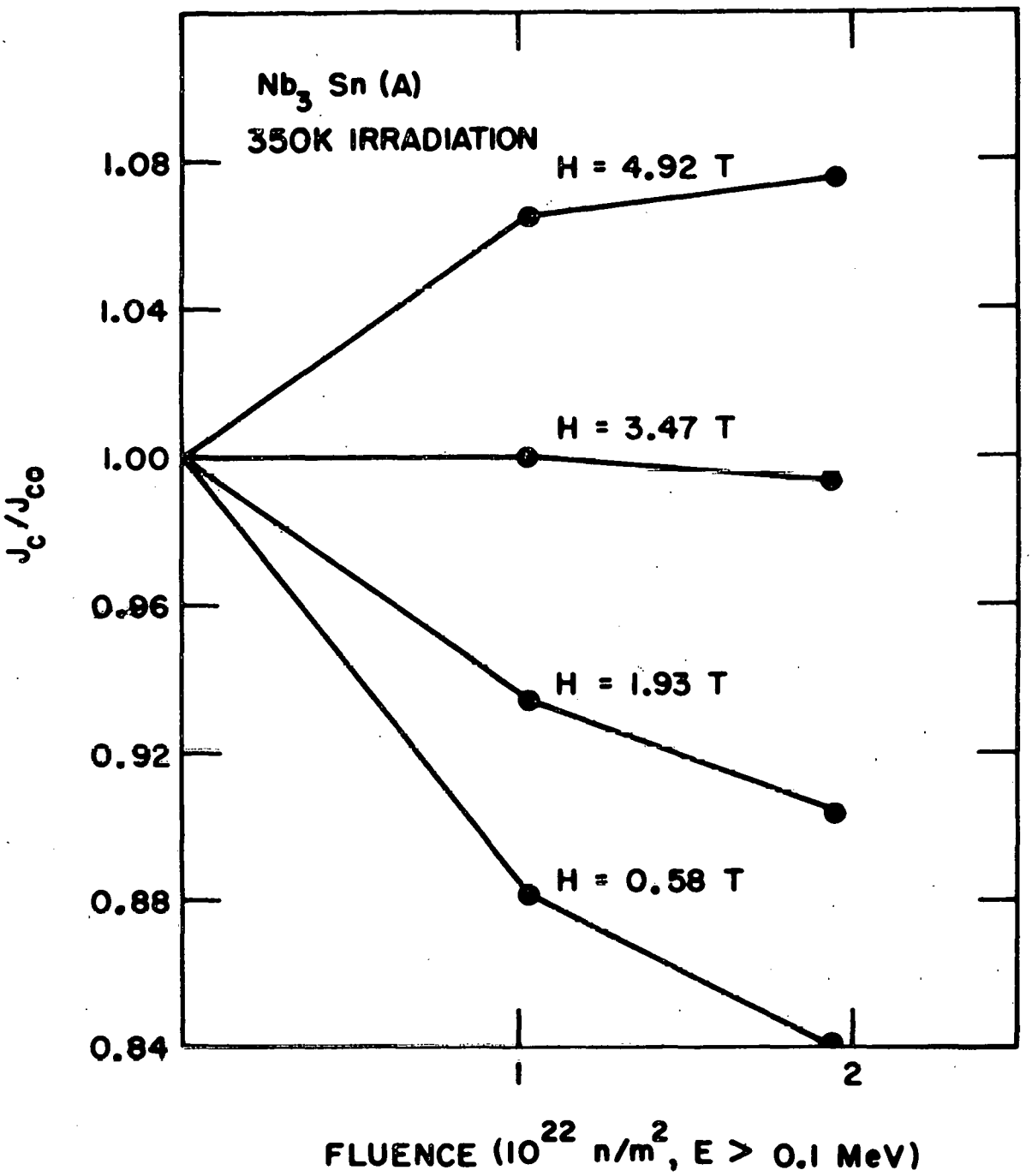

Figure I-16. Change in J_c for high J_{co} material during 350 K irradiation.

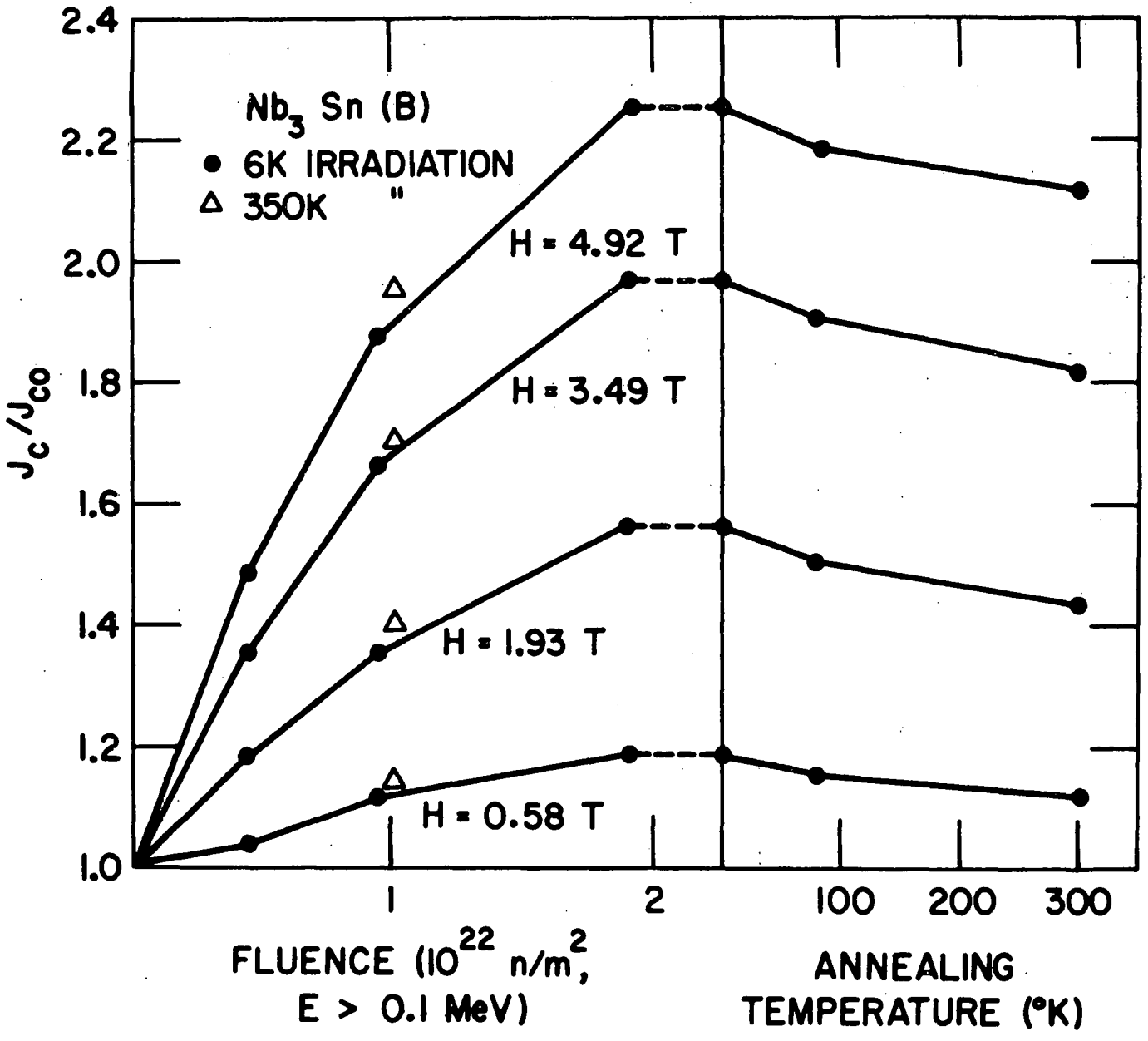

Figure I-17. Change in critical-current density for low J_{co} material during 6 (●) and 350 K irradiations (△).

The effect of J_{co} on the J_c changes after 6 K irradiation is observed more easily in Figure I-18. The J_c changes in samples A and B as well as a previously reported sample (with a J_{co} between A and B) are plotted versus field and dose. As J_{co} increases, the radiation-induced enhancement in J_c becomes smaller. This is observed for all fields, and only two values of H are presented here for clarity.

The results of these experiments show that both the initial sample metallurgy and the irradiation temperature play important roles in determining the J_c changes during neutron irradiation. The design data necessary for fusion magnets will require irradiation below 10 K of the material to be used in the magnet (presumably high J_{co} material). This effect of J_{co} and irradiation temperature on the J_c changes during fast-neutron irradiation were also observed (but to a lesser extent) in NbTi and should be considered in radiation damage experiments of the other magnet components, such as the insulators and composites.

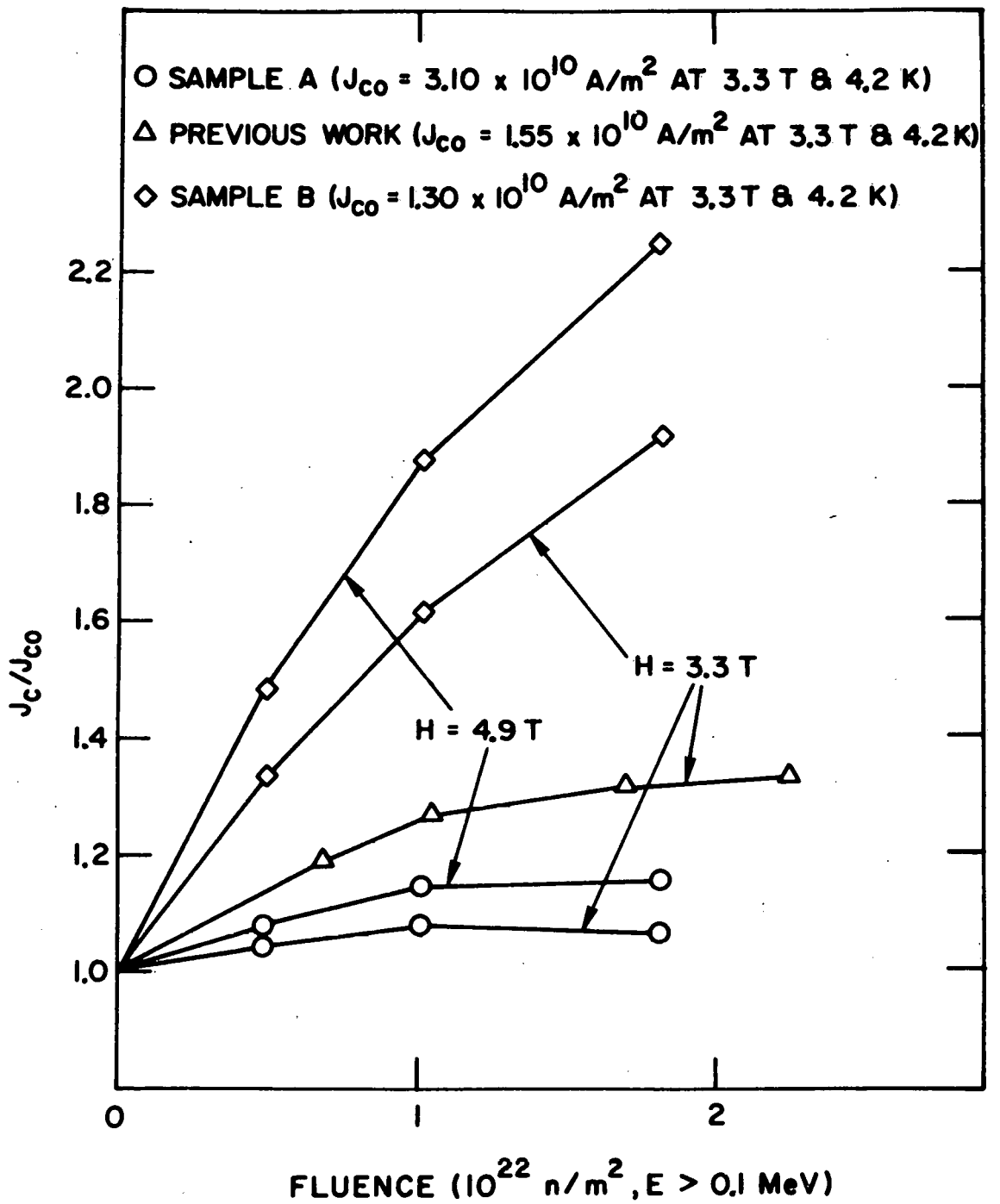

Figure I-18. Changes in J_c vs field and dose for samples with different J_{co} (A, B, and a previous irradiation[11]).

II. EXPERIMENTAL POWER REACTOR

A. First-Wall/Limiter Design

D. L. Smith, Materials Science Division

The focus of the present study is the integrated design of a first-wall/limiter system for a tokamak Experimental Power Reactor (EPR). Although a limiter is used in nearly all presently operating fusion devices, the design aspects of a limiter for power reactors have received only cursory attention. A major problem is caused by the deposition of high cyclic heat fluxes on the plasma-side surfaces of the first-wall system. For a reactor operating without a divertor, the surface heat flux is equivalent to ~ 25% of the neutron wall loading. About 40% of the surface heat flux (or 10% of the neutron wall load) is in the form of electromagnetic radiation, with the remaining 60% (15% of the neutron wall load) attributed primarily to ion and electron transport. A small fraction of the transport losses may come from neutrals.

The present first-wall design concept utilizes multiple (up to 16) radiatively-cooled poloidal limiters. The maximum number, which corresponds to the number of toroidal-field coils, may effectively cover 20-25% of the first wall. All of the ion and electron transport losses from the plasma are assumed to be deposited on the limiters while the radiation losses are assumed to be distributed uniformly to the limiter and first wall as a function of the exposed surface area. The larger number of limiters tends to reduce the net heat load to each limiter. The limiter is assumed to radiate its heat to the the water-cooled first wall from its front surface as well as the back surface. For similar effective surface heat fluxes, thermal radiation from the front surface should reduce the thermal gradient through the limiter compared to the thermal gradient predicted for the complete radiatively-cooled liner that effectively radiates only from its back surface. Also, because of the thermal inertia provided by the limiters, thermal radiation from the limiters to the metal wall during the off part of the burn cycle will tend to reduce the extent of thermal cycling in the water-cooled first wall. It is anticipated that proper selection of the number and size of the limiters will reduce the cyclic thermal stresses, and hence increase the lifetimes, of both the limiters and the first wall. Calculations for the thermal responses of both the limiters and first-wall are being conducted for power cycles and wall loadings expected for the EPR.

B. Impurity Control Studies

J. N. Brooks, Applied Physics Division

During the previous quarter the role of a limiter/first-wall/vacuum port system was identified as a potential impurity control system for EPR.[1]

[1] C. C. Baker, et al., "Fusion Power Program Quarterly Progress, July-September, 1977," Argonne National Laboratory, ANL/FPP-77-4 (1977).

A detailed parametric model of the interaction between the plasma and a limiter system has now been developed and has been used to analyze the requirements of such a system. The model treats the processes of sputtering by charged particles at the limiter and by neutrals at the wall, reflection of particles from the limiter and wall and pumping of particles at the vacuum port. As an impurity control device the limiter system could operate in three ways: (1) some of the sputtered, low-Z impurity atoms from the limiter are directed to the wall and/or a vacuum port where they tend to stick or be pumped, (2) some of the low-Z ions and the He ions from the plasma impinging on the limiter are reflected to the wall and/or vacuum port in the same way as the sputtered material, and (3) the limiter directly retains some of the He impinging on it. These three cases and combinations thereof have been studied using the model and the plasma burn cycle code. The results seem to show significant potential for this technique as an impurity control device. Modest performance parameters, e.g. 85% reflection of particles from the limiter back to the plasma and only 15% away from the plasma, increase the net power production significantly, and a more demanding but still probably feasible parameter of 50% reflection to the plasma and 50% away approaches the performance obtainable with a divertor. A key question, however, is whether any type of limiter can withstand the large heat flux from a reactor such as EPR; this topic is under investigation (see above).

C. Refueling

D. Ehst, Applied Physics Division

A study of pellet injection into the EPR plasma was initiated, using the pellet ablation model of Parks, et al.[1] Their ablation formula was evaluated for temperature and density profiles typical of the EPR,

$$n_e(x) = n_{eo}\left[1 - \left(\frac{x}{a}\right)^2\right]^{\alpha_n}$$

and

$$T_e(x) = T_{eo}\left[1 - \left(\frac{x}{a}\right)^2\right]^{\alpha_T},$$

to yield

$$r^{2/3}\,\dot{r} = 5.85 \times 10^{-5}\left[1 - \left(\frac{x}{a}\right)^2\right]\frac{\alpha_n}{3} + \frac{7\alpha_T}{6} + 0.549\,\alpha_T\,,$$

where r is the fuel pellet radius. Taking the pellet trajectory to be $x = a - vt$, this expression was analytically integrated for the EPR profiles $\alpha_n = 0.3$ and $\alpha_T = 1.1$. From the resulting r(x) the ablated fuel at each point of minor radius was found, and dividing by the differential flux surface volume, $V'\Delta\psi$, the fuel density was found to be

---

[1] P. B. Parks, R. J. Turnbull and C. A. Foster, *Nuclear Fusion*, 17, p. 539 (1977).

$$n_f(x) = \frac{1.932 \times 10^{21}}{\frac{dV}{d\psi}\,\frac{d\psi}{dx}}\; r_0^3\, A \left[1 - \left(\frac{x}{a}\right)^2\right]^2 \left[1 + AF\left(\frac{x}{a}\right)\right]^{-4/5} .$$

Here $$A = \frac{9.647 \times 10^{-5}\, \bar{n}_e^{1/3}\, \bar{T}_e^{1.715}}{r^{5/3}\, v} ,$$

r_0 = initial pellet radius, v = pellet speed,

$$F(y) = y - \frac{2}{3}y^3 + \frac{y^5}{5} - \frac{8}{15} ,$$ and all units are c.g.s.

Using the flux surfaces $\psi(x)$ and volume metric V' for the EPR, the injected fuel density was computed for various combinations of r_0 and v. The deposition profiles were generally peaked towards the outside of the plasma when $\bar{n}_e = 1.43 \times 10^{20}$ m^{-3} and $\bar{T}_e = 8$ keV, even for optimistic pellet acceleration schemes. For example, a pellet of radius $r_0 = 0.4$ cm traveling at $v \approx 1.5 \times 10^4$ cm s^{-1} could achieve A = 4.11 and penetration half-way into the plasma provided Park's[1] model is modified to include fuel ionization in fusion plasmas. This is well beyond the capabilities of present-day injectors. Moreover, such a pellet would increase the DT density by 35% over an abrupt time period, and three or four such pellets would be required for a 60-s EPR burn cycle.

During the burn $\bar{T}_e$ and $\bar{n}_e$ will decrease, which allows better pellet penetration, so a dynamic calculation was done by Jeff Brooks with pellets injected at widely spaced ($\sim$ 15 s) intervals. Unfortunately, $\bar{n}_e$ and $\bar{T}_e$ do not decrease sufficiently to allow better penetration; the large cold fuel increases tend to quench the burn.

We conclude that bare fuel pellet injection alone is not likely to yield centrally-peaked fuel densities for EPR with the technology available in the near future.

37-46

04391

III. FUSION SYSTEMS ENGINEERING

A. Fusion Reactor Systems Studies

M. A. Abdou, Applied Physics Division

Significant progress has been made in this quarter in achieving the goals of the fusion reactor systems studies for FY 1978. Among these goals are: (1) upgrading the ANL systems code for tokamak power plants in both areas of performance and costing analyses, and (2) documenting the code and issuing a user's manual.

The executive routine of the systems program was converted from PL-1 to the FORTRAN programming language. This was found necessary to ensure the "expertability" of the code to other interested organizations. While the PL-1 language offers unique features for parameter sweep and optimization capability, it is not acceptable by some computers such as the CTR-Livermore machine.

Significant revisions were made in the various performance and costing models of the system code for tokamak power plants. A summary of the developments for the vacuum, tritium and neutral beam injectors subsystems is given below.

1. Tritium and Vacuum Subsystems

R. G. Clemmer, Chemical Engineering Division

The principal objective of this study for FY 1978 is to adapt the tritium and vacuum subsystems code (TCODE) to the ANL systems code for tokamak power plants. TCODE was originally put together to support "The Next Step" (TNS) design studies conducted during FY 1977.[1] During the first quarter of FY 1978, the earlier version of TCODE was upgraded to include additional parametric functions and more detailed costing algorithms. Further, the upgraded form of TCODE (version III) is applicable to commercial reactors with breeder blankets and divertors as well as to near-term experimental devices. A selected sample of the 60 input parameters and 100 output parameters for some near-term (ITR,[2,3] TNS,[2,3] EPR[4]) and commercial (UWMAK

---

1 C. C. Baker, et al., "Fusion Power Program Quarterly Progress Report: July-September, 1977," Argonne National Laboratory, ANL/FPP-77-4 (1977).

2 C. C. Baker, et al., "TNS Scoping Studies, Interim Status Report: October 1976-March 1977," General Atomic Company Report GA-A14412, and Argonne National Laboratory Report ANL/FPP-77-2 (May, 1977).

3 ANL Project Staff, "GAC-ANL TNS Scoping Studies: Volume V, Support Engineering, Tritium and Neutronics," Argonne National Laboratory, ANL/FPP-77-6, and General Atomic Company, GA-A14614 (January, 1978).

4 W. M. Stacey, Jr., et al., "EPR-77: A Revised Design for the Tokamak Experimental Power Reactor," Argonne National Laboratory, ANL/FPP/TM-77 (March, 1977).

series[5-7]) reactor designs is shown in Table III-1. Also included in the table are parameters for a hypothetical reactor (UWMAK-III M) having similar characteristics to UWMAK-III but a higher fractional burnup (5.0% versus 0.83%). Studies of the sensitivity of tritium systems to plasma and operating conditions for near-term reactors have been previously described.[8,9] A summary of the major results obtained from the revised code, based largely on Table III-1, is given below.

The torus evacuation system is assumed to have compound cryopumping, i.e., cryocondensation pumping for hydrogenic species (DT) and cryosorption pumping of helium. The code separately calculates pumping speeds for the two types of species. For reactors having no divertor, the torus vacuum pumps were assumed to operate only between burn pulses. The duct conductances for helium pumping were assumed to be reduced by a factor of one-third because of the presence of condensation surfaces ahead of the cryosorption panels. It was a significant finding that, for a near-term reactor without a divertor and with large fractional burnup (> 10%), the required speed for helium pumping is very high (from one to six times the required DT pumping speed). The required helium pumping speeds for commercial reactors with divertors are very high but rather insensitive to fractional burnup. By contrast, required DT speeds are very sensitive to fractional burnup (FB), with UWMAK-III (FB = 0.83%) having a required DT speed in excess of 10^5 m^3/s. The neutral beam vacuum system requirements and costs are relatively insensitive to overall reactor design. The design of the neutral beam injectors for EPR had a higher gas efficiency than that for either ITR or TNS, therefore, pumping speeds and costs were lower. The beam vacuum systems for commercial reactors are similar in size and cost to those of near-term reactors. (UWMAK-III does not use neutral beam heating). One significant point is that while near-term reactors will likely have mass flow rates of deuterium in the neutral beam recycle comparable to or greater than those of the fuel cycle, commercial reactors (due to their long burn times and fewer total burns per day) will have considerably lower neutral beam recycle rates. Further, the

---

5 B. Badger, et al., Fusion Feasibility Study Group, "UWMAK-I, A Wisconsin Toroidal Fusion Reactor Design," Nuclear Engineering Department, University of Wisconsin, UWFDM-68 (March, 1974).

6 B. Badger, et al., "UWMAK-II, A Conceptual Tokamak Fusion Reactor Design," Nuclear Engineering Department, University of Wisconsin, UWFDM-112 (1975).

7 B. Badger, et al., "UWMAK-III, A Noncircular Tokamak Power Reactor Design," Nuclear Engineering Department, University of Wisconsin, UWFDM-150 (1976).

8 R. G. Clemmer and W. F. Calaway, "Impact of Plasma Performance Parameters upon the Vacuum and Tritium System Design Requirements for Near-term Tokamak Reactors," presented at the International Atomic Energy Agency Conference and Workshop on Fusion Reactor Design, Madison, Wisconsin (October 10-21, 1977).

9 J. M. Mintz, R. G. Clemmer and V. A. Maroni, "Tritium Handling Trade Studies and Design Options for the GA/ANL TNS," Proc. of the Seventh IEEE Symposium on Engineering Problems of Fusion Research, Knoxville, Tennessee (October 25-28, 1977).

Table III-1. A Selected Sample of Results From TCODE

TCODE-Version III Selected Parameter List.	GA/ANL ITR	GA/ANL TNS-UP	ANL EPR	UWMAK I	UWMAK II	UWMAK III	UWMAK III M
*Burn Time (s)	30.	90.	64.	5400.	5400.	1800.	1800.
*Dwell Time (s)	270.	30.	16.	390.	330.	100.	100.
*Thermal Power (MW)	390.	465.	325.	5000.	5000.	5000.	5000.
*Ion Density (Ions/m^3)/10^{20}	1.48	1.40	1.30	0.75	0.75	0.79	0.79
*Particle Confinement Time (s)	1.63	1.54	5.00	8.28	8.28	0.55	(2.5)
*Divertor	no	no	no	yes	yes	yes	yes
*Fractional Burnup, FB	0.124	0.187	0.161	0.050	0.0485	0.0083	(0.050)
*Evacuation Volume (m^3)	314.	443.	450.	7000.	7000.	2600.	2600.
*Number of Vacuum Pumps (Operating/Total)	3/6	12/24	12/24	(Divertor)	(Divertor)	(Divertor)	(Divertor)
Required Pump Capacity (kPa-m^3)	2.77	4.11	7.36	1.48×10^4	1.48×10^4	1.87×10^4	3.61×10^3
Required DT Pump Speed (m^3/s)	2.37	16.62	37.06	8.11×10^4	8.12×10^4	1.07×10^5	1.98×10^4
Required He Pump Speed (m^3/s)	2.67	90.96	232.	8.53×10^3	8.28×10^3	1.79×10^3	2.08×10^3
Cryopanel Surface Area (m^2)	0.053	1.82	4.64	171.	166.	35.9	41.6
Cost-He Sorption Pumping ($M)	0.012	1.6	4.2	12.8	12.4	2.7	3.1
Cost-DT Condensation Pumping ($M)	0.01	0.1	0.1	48.6	48.7	64.3	11.9
Cost-Cryopump Regeneration ($M)	0.01	0.03	0.1	25.6	25.6	32.4	6.2
Cost-Hard Seal Metal Valves ($M)	0.27	1.1	1.3	9.6	9.4	2.8	3.1
Tritium Input (gas), (g/day)	27.2	84.4	126.	18.0	18.2	21.3	21.3
Tritium Pellet Fueling (g/day)	20.9	201.	121.	1.25×10^4	1.21×10^4	7.07×10^4	1.17×10^4
Tritium Burnup (g/day)	6.0	53.3	39.8	624.	587.	587.	587.
Total Tritium Inventory (kg)	0.26	1.81	1.36	38.9	28.8	82.1	28.9
Annual Tritium Consumption (kg)	0.45	14.7	9.15	-92.8	-9.32	-43.7	-44.0
Deuterium Injected (g/day)	12.0	29.9	51.1	1.36	0.88	0.0	0.0
Deuterium Pumped in Injectors (g/day)	77.6	194.1	81.0	4.21	2.71	0.0	0.0
Tritium Backstream to Beam Pumps (g/day)	0.42	1.04	2.60	0.19	0.19	0.0	0.0
*Number of Injectors	6	6	12	16	16	0	0
Beam Pump Speed (m^3/s)	3360.	3360.	820.	1600.	1600.	0.0	0.0
Beam Getter-Pump Surface Area (m^2)	146.	146.	35.6	69.6	69.6	0.0	0.0
Maximum Conceivable Release, MCR (g)	67.5	189.0	144.8	8730.	8325.	47500.	8140.
Building Volume (m^3)/10^5	0.6	0.6	0.6	13.6	5.0	1.0	1.0
*E.D.S. Cleanup Time (hr.)	48.0	48.0	48.0	48.0	48.0	48.0	48.0
E.D.S. Flow rate (m^3/s)	4.31	4.67	4.58	124.3	46.5	10.7	9.68
Tritium Stacked to Environment (Ci/MCR)	3.00	3.00	3.00	13.6	10.0	5.00	5.00
Tritium Vented to Environment (Ci/MCR)	0.15	0.39	0.30	15.3	14.3	70.9	13.5
Cost-Tritium Recovery ($M)	0.0	0.0	0.0	2.1	5.7	3.7	3.7
Cost-Fuel Processing ($M)	4.9	7.3	6.8	35.3	38.5	78.9	36.0
Cost-E.D.S. ($M)	5.6	6.0	5.8	133.	50.2	12.4	11.3
Cost-Torus Evacuation ($M)	0.3	2.8	5.7	96.6	96.1	102.	24.3
Cost-Neutral Beam Vacuum System ($M)	42.3	42.3	20.7	53.8	53.8	0.0	0.0
Total Cost: Tritium and Vacuum Systems ($M)	53.0	58.4	39.0	320.	244.	197.	75.2

*Input Parameters

amount of deuterium required to feed the neutral beams is less than that burned. As a consequence of this, the isotopic separation system for a commercial reactor may be simpler than that required for a near-term experimental reactor, because the high purity deuterium feed for the neutral beams could be supplied directly from an external source without recycle.

An item of considerable significance from the standpoints of both safety and costs is the emergency air detritiation system (EDS). The costs of such systems are primarily due to the reactor building volume and the permissable cleanup time. Our earlier studies[9] indicated that the cleanup time should be no longer than about 48 hours. The required speed to attain this is about 0.5% of the reactor building volume per minute. Further, since the unit costs are about \$20,000 per m^3/min, the cost of the EDS is about \$100 per m^3 of reactor building. Since this is about half the cost of the reactor building itself, the EDS is a significant cost driver.

Finally, a comparison of UWMAK-III and UWMAK-III M (Table III-1) serves to measure the effect of fractional burnup (which in turn is a strong function of the particle confinement time). This comparison shows that there are considerable economic and safety incentives for trying to increase the fractional burnup of commercial scale tokamak reactors. (Increasing the fractional burnup dramatically lowers tritium inventories, potential tritium releases and overall costs.)

2. Neutral Beam Injector Model

D. Ehst, Applied Physics Division

The new neutral injector calculational model is based on various designs developed at ANL for TNS and EPR size devices.[3,4] Basically, the injector consists of a source of positively ionized energetic deuterium atoms and molecules followed by a bending magnet to remove the unwanted molecular species and then a neutralizing cell and a second magnet to remove any unneutralized deuterons before the beam passes into the tokamak chamber. Both electrical and thermal energy are recovered from the deflected charged particles. This model contains detailed calculations of beam transport, gas loads and power flow.

The model is organized as follows: (1) from an initial guess of the beam attenuation the ion source requirements are determined; (2) the beam width and location of the beam waist (focal point) are computed; (3) the neutralizer cell width matches the beam width and the required gas flow for neutralization is found; (4) the gas loads into various chambers are computed; (5) the particle line densities and beam attenuation are derived from the pressure distribution along the beam line. At this point the whole previous calculation is iterated until the beam attenuation converges; and finally, (6) the power flow and efficiency are calculated.

B. Development of Blanket Processing Technology for Fusion Reactors

The program under way in the Chemical Engineering Division to initiate the development of processing technology for liquid lithium fusion reactor blankets is continuing. Progress during the first quarter of FY 1978 is summarized below.

1. Lithium Processing Test Loop (LPTL)

J. R. Weston and V. A. Maroni, Chemical Engineering Division

Construction work on the LPTL was completed by early December and the loop was filled with lithium in mid-December. Approximately 99 kilograms (∿ 200 liters) of lithium were transferred from a specially constructed stainless steel carboy into the LPTL dump tank. During the transfer operation, the carboy and dump tank were heated to 250°C and the transfer line was heated to 300°C. The transfer was accomplished by pressurizing the carboy to ∿ 3 psig with argon while the dump tank was maintained at ∿ 1 psig (argon). The entire transfer took ∿ 2-1/2 hours and no problems were encountered.

The lithium was supplied by the Lithium Corporation of America (Lithcoa). (They had filled the carboy at their Bessemer City, North Carolina plant in late September.) To date nearly a dozen samples have been taken from the LPTL reservoir tank, and broad spectrum chemical analyses of several of these samples are in progress to verify the assay provided by Lithcoa.

During LPTL startup, piping and vessel temperatures were raised to ∿ 350°C and the EM-pump channel was heated to ∿ 500°C. Some early problems were encountered with freezeup in the pump channel and with trapped gas bubbles cavitating the pump (MSA Style V). On some occasions back-flowing of the pump, by operating the dump valve, freed the gas bubbles from the pump channel. On other occasions, it was necessary to completely dump and refill the entire system. As a result of a combination of factors, recent startups have been made without difficulty. Firstly, we now evacuate the reservoir tank and lines prior to filling; secondly, the system is probably fairly well broken in ("wetted") by now; and thirdly, we have made some modifications to the pump itself to include additional heating, insulating and temperature monitoring capability along the pump channel. The latter step (i.e., pump modification) was believed to have had the most to do with relieving startup problems, and will probably be necessary on any lithium system using an EM-pump originally designed for sodium service.

As of the time of this writing, the LPTL had operated at ∿ 380°C for over 400 hours without any evidence of problems. The LPTL is presently flowing in both the bypass and getter-trap/cold-trap branches at rates of 0.5 to 1.0 gallon/min (in each branch). During the second quarter of FY 1978 the loop temperature will be raised to 460-480°C, and initial tests of hydrogen meter and cold trap performance will be made. The hydrogen meter tests will be done using deuterium to reduce background effects. The cold trap tests

will be performed by making step-wise reductions (∿ 20°C per step) in cold-trap temperature and withdrawing samples from the reservoir tank for analysis. Analyses for N, O, Fe, Cr, Ni and Zr will be made in the early stages.

2. Supporting Studies

R. M. Yonco and V. A. Maroni, Chemical Engineering Division

An apparatus was developed for taking samples of liquid lithium from the reservoir of the LPTL. A fritted sample tube, attached to the end of a threaded sampling shaft, is coupled to the reservoir tank through one of three sampling ports built into the upper dished end-head. The tube is lowered into the reservoir tank until an electrical signal indicates that the tube is immersed in lithium. Vacuum is applied through the sampling shaft until the filtered lithium rising in the tube contacts an electrical probe. The sample tube is then withdrawn from the sample port and the threaded end of the tube is sealed with a pinch-off tool. Eleven samples were taken during the first month of loop operation.

Work on the glass mock-up of the LPTL salt tank is also continuing. The micro-processer driven control circuit has been fully developed and checked out. Tests of phase mixing and separation using organic and aqueous solutions (to simulate the salt and lithium, respectively) will start during the second quarter on FY 1978. Plans are being made to prepare a short motion picture of the operating sequence of the salt tank mock-up.

C. Safety Studies of Fusion Concepts

1. Analysis of Tritium Soaking Mechanisms

R. G. Clemmer and V. A. Maroni, Chemical Engineering Division

This project has involved a series of coordinated studies[1,2] aimed at developing a basis for understanding the effects of selected reaction and soaking mechanisms on large-scale air detritiation operations. A computer code (TSOAK) has been formulated to model these mechanisms[1,2] and a small-scale

---

[1] C. C. Baker, et al., "Fusion Power Program Quarterly Progress Report, July-September, 1977," Argonne National Laboratory, ANL/FPP-77-4 (1977).

[2] R. G. Clemmer, R. H. Land, V. A. Maroni and J. M. Mintz, "Simulation of Large-Scale Air-Detritiation Operations by Computer Modeling and Bench-Scale Experimentation," Argonne National Laboratory, ANL/FPP-77-3 (November, 1977); also, published in abridged form in the Proceedings of the Seventh IEEE Symposium on Engineering Problems of Fusion Research, October 25-28, 1977, Knoxville, Tennessee, IEEE Publication Number 77CH1267-4-NPS (1977).

experimental apparatus has been set up to test selected features of the model.[1,2] During the first quarter of FY 1978 a detailed report[2] describing the results of FY 1977 activities was completed and forwarded for publication.

The scope of work for the present fiscal year includes continued experimental studies with the bench-top enclosure and upgrading of the computer code TSOAK. These studies are scheduled to begin during the second quarter of FY-1978. In preparation for their initiation, a new tritium monitor was ordered from Overhoff and Associates and is due to arrive in early March. (The previously used monitor was manufactured by Johnston Laboratories.) The Overhoff monitor is the type selected for use at PPPL for the Tokamak Fusion Test Reactor (TFTR) and at LASL for the Tritium Systems Test Assembly (TSTA). As part of the first series of experimental runs, the two monitors will be tested in tandem to determine their reproducibility and the extent to which monitors of this basic type are subject to "memory" effects.

Another area of concern relates to the achievable efficiency of scrubber systems for emergency detritiation units. In particular, there is considerable incentive to operate the tritium oxidation-catalyst at as low a temperature as possible, but existing data[3,4] indicate a temperature above about 300°C may be required to obtain the desired decontamination factors (i.e., on the order of 10^6).[5] It is planned to investigate the behavior of a number of commercially available catalysts as a function of temperature, inlet concentration of tritium and hydrogen and flow rate using the bench-top enclosure.

In addition to the investigations of scrubber system and monitor performance, steps will be taken to upgrade the computer code TSOAK in order to more precisely account for diffusion effects at times late in the cleanup operation. The code will then be used to analyze the results of bench-scale experiments that are representative of the latter stages of cleanup operations.

---

[3] J. C. Bixel and C. J. Kershner, "A Study of Catalytic Oxidation and Oxide Absorption for the Removal of Tritium from Air," Proceedings of the Second AEC Environmental Protection Conference, Albuquerque, New Mexico, April, 1974, p. 261.

[4] T. R. Galloway, Lawrence Livermore Laboratory, personal communication.

[5] M. E. Muller, Los Alamos Scientific Laboratory, personal communication.

D. The MACK/MACKLIB System for Nuclear Response Functions

M. A. Abdou and Y. Gohar, Applied Physics Division

A primary function of the neutronics analysis for fusion reactors is to estimate a set of nuclear response rates. The calculation of a nuclear response involves an integration over the appropriate phase space of the product of the neutron (or gamma) flux and a nuclear response function. Examples of the latter are tritium production cross section, neutron kerma factor,

gas production cross section and atomic displacement function. The original version of the MACK computer program[1] was developed to calculate the nuclear response functions of importance in fusion applications from basic nuclear data in ENDF/B[2] format. Recently, major developments have been made in the calculational algorithms and new capabilities have been added into the MACK code. The new version of the code has been released as MACK-IV.[3]

An important part of the MACK program concerns the calculation of the neutron kerma factor, which can be expressed for any nuclide at any neutron energy as

$$k_n = \sigma_t E + \sum_i \sigma_i Q_i + \sum_{i'} \sigma_{i'} E_{Di'} - \sum_m \sigma_m \bar{E}_{n',m} - S^*_{E\gamma} , \qquad (1)$$

where σ_t is the total cross section; Q_i is the energy resulting from mass conversion in reaction i; $E_{Di'}$ is the average decay energy per reaction i'; $E_{n',m}$ is the average secondary neutron energy per reaction m, and $S^*_{E\gamma}$ is the total gamma energy emitted from all reactions per unit flux. The calculation of the last term, $S^*_{E\gamma}$, is involved and is a key item in the work described here. This term can be calculated by the new version of the program, MACK-IV, via one of two paths as selected by the user:

(1) The Nuclear Kinematics Path: In this path, the solutions of the kinematics equations of all nuclear reactions are used to calculate $S^*_{E\gamma}$. The expression for $S^*_{E\gamma}$ is only a function of the neutron reaction cross section and the secondary neutron (and charged particles, if any) energy and angular distribution. Thus, in this methodology no direct information on gamma production is required.

(2) The Gamma Production Path: In this path, $S^*_{E\gamma}$ is calculated directly from the gamma production data as

$$S^*_{E\gamma}(E_n) = \int \sigma_p(E_n, E_\gamma)\, E_\gamma\, dE_\gamma , \qquad (2)$$

where $\sigma_p(E_n,E_\gamma)$ is the production cross section for a photon with energy E_γ at an incident neutron energy E_n.

---

[1] M. A. Abdou, C. W. Maynard and R. Q. Wright, "MACK: A Program to Calculate Neutron Energy Release (Fluence-to-Kerma Factors) and Multigroup Neutron Reaction Cross Sections from Nuclear Data in ENDF Format," Oak Ridge National Laboratory, ORNL-TM-3994 (1973); also University of Wisconsin, UWFDM-37 (1973).

[2] D. Garber, C. Dunford and S. Pearlstein, "Data Formats and Procedures for the Evaluated Nuclear Data File, ENDFs," BNL-NCS-50496; also ENDF-102 (1975).

[3] M. A. Abdou, M. Y. Gohar and R. Q. Wright, "MACK-IV, A New Version of MACK: A Program to Calculate Nuclear Response Functions from Data in ENDF Format," Argonne National Laboratory, ANL/FPP-77-5 (1978).

The gamma production path was not provided in the earlier version of MACK because of the lack of the gamma production data at that time. This data have been provided for a large number of materials in ENDF/B-IV to warrant the new development. The nuclear kinematics path has been retained and improved in MACK-IV because: (1) gamma production data is still lacking for some important materials (e.g. ^{11}B); and (2) it provides a convenient way for calculating the contribution to heating from each individual reaction that is of interest in specialized nuclear and chemonuclear applications.

A new processor is included in MACK-IV to calculate the gamma production cross sections and the gamma production energy matrix. These are needed to compute $S^*_{E\gamma}$ in Eq. (2) but there are other important reasons to calculate the gamma production cross sections in MACK. From physics standpoint, the gamma production data are strongly related to the neutron interaction data through the principle of energy conservation. Processing the neutron kerma factors simultaneously with the gamma production data permits a consistent methodology to be employed in both types of calculations and ensures that the energy is preserved in the computation of nuclear heating. The neutron interaction and gamma production information are not consistent in the current data evaluations for many materials. The new procedure in MACK-IV provides an adequate basis for data adjustment and for incorporating theoretical models to compensate for the lack of some data.

A new processor has been incorporated into MACK-IV to calculate the neutron kerma factors from fission to permit accurate calculations of nuclear heating in hybrid fission-fusion reactors. An evaluation of present methods employed for fission reactor heating calculations reveals that a host of poor approximations are commonly employed. By providing kerma factors for fissionable materials a new step has been undertaken not only to improve the nuclear heating calculations in hybrid reactors, but also to provide a long needed methodology for accurate calculations of the power distribution in fission reactors. Other features of MACK-IV include an improved treatment of the cross section calculations in the resonance region and generalized energy mesh, energy group structure and response function weighting options.

The validation of the MACK-IV results were performed using the direct energy balance method[4] as applied to typical fusion reactor systems. The major difficulties with the data evaluations in Version IV of ENDF/B can be classified into three broad areas: (1) the lack of data by isotope for naturally occurring elements with more than isotope; (2) the lack of cross sections for some specific reaction types; and (3) inconsistencies among various types of data (most notably between the neutron interaction and the gamma production files), particularly as to preserving the energy.

MACK-IV is currently being employed to generate a new library, MACKLIB-IV, of response functions from ENDF/B-IV for a large number of materials that are presently of interest in fusion reactor applications. The library is in the

[4] M. A. Abdou and C. W. Maynard, *Nucl. Sci. Eng.*, 56, p. 360 (1975).

CTR energy group structure[5] of 171 neutron groups and 36 gamma groups. The library can be directly used with current transport codes and includes neutron and gamma kerma factors; tritium, helium and hydrogen gas production functions, other reaction cross sections and atomic displacement functions. Additional details about MACKLIB-IV will be given in the next progress report.

---

[5] R. W. Roussin, et al., "The CTR Processed Multigroup Cross Section Library for Neutronics Studies," Oak Ridge National Laboratory, ORNL/RSIC-37 (1977).

E. Energy Storage and Power Supply Systems for Fusion Reactors

J. N. Brooks and K. Evans, Jr., Applied Physics Division

A 7-m tokamak reactor design description has been developed for use as a basis for the power supply study project for this year. This reactor has a 2500-MWth output, an air core OH transformer and an externally located superconducting EF system. Options for the EF coil locations have been extensively studied using the recently developed EFC code. By a judicious choice of EF coil locations and currents, it appears that the total EF stored energy can be substantially reduced over previous estimates, to about 2.0 GJ, down from 4.5 GJ. Burn cycle studies are underway to analyze the impact of several potential cost saving operating techniques. Based on preliminary results, a large reduction in the plasma resistive loss during startup can be achieved if the amount of oxygen in the plasma can be kept low. The reduction in EF stored energy and in plasma resistive loss both imply large cost savings. It is planned to quantify these cost savings using the upgraded cost algorithms currently being developed by ANL/Accelerator Research Facilities Division personnel.

IV. MAGNETIC SYSTEMS

A. Energy Storage and Transfer Program

R. L. Kustom, R. Wehrle, R. P. Smith and R. Fuja, Accelerator Research Facilities Division

The energy storage and transfer systems described in previous Fusion Power Program Quarterly Reports are undergoing updating modifications to allow for more accurate evaluation. Problems plaguing the homopolar generator (Hope I) center around the brushes and the brush guide ring. As mentioned in previous reports the brush area had been increased and the brush collecting straps changed (to a soft copper) to allow for freer movement of the brushes. Since the brush guide rings were made of brass, we were concerned that they were not an equal potential surface, so a layer of teflon tape was wrapped around the ring. With these changes the system was assembled and tested, the results of the test were:

1. The teflon tape came loose and lodged between the cylindrical drum and the brush guide ring, and

2. We were not able to pass currents above 60 amperes dc without losing our current path through the drum.

However, at the start of the tests we were able to obtain good agreement with theory between drum voltage and drum speed.

The brush guide ring was removed and a teflon layer was epoxy-bonded to the brush guide ring surface. While the bonding was taking place, four search coils, each with 4000 turns of number 44 wire, were wound to try and determine the effects of drum eddy currents on the radial magnetic field during acceleration and deacceleration of the generator. The modifications have been completed and the system reassembled, testing will resume in a few days. If the teflon bonds hold, the problem with the current path opening at high speeds and large currents will be investigated. If all goes well, energy will again be transferred from the storage inductor to the homopolar generator.

Modification to the energy switching circuits have also been performed allowing for easier operation of the switching cycle. Improvements have also been completed on the drum speed measuring circuits.

The controlling circuits for the inductor-converter (IC) bridge are undergoing major changes to allow for variable energy transfer and control. An Intel system 80/20 microprocessor is being programmed to perform the energy control function. The programs needed have been written and are being debugged on the microcomputer. The input and output interface circuits, for the microcomputer, have been designed and parts needed for their construction are on order. The output interface circuits are built and working, with the input circuits remaining to be assembled. Testing of the IC bridge with the new controls will resume as soon as possible.

B. Negative Ion Source Development

J. A. Fasolo, Accelerator Research Facilities Division

An external cesium boiler and a cesium transfer line have been designed and built for the Penning-type cesium-activated surface plasma source. A freon-cooled jacket for the pulsed gas valve has been designed and is under construction. The valve and the source are mounted in vacuum. Valve cooling will allow the use of an O-ring sealed coupling between the valve and the source body and eliminate by-pass leakage due to the presently used slip-fit coupling. The new coupling is being built.

Work on a housing for the source is nearing completion. A high-voltage enclosure has been built and an SCR-controlled arc modulator is being assembled and installed. A regulated dc high-voltage supply has been assembled.

Work on the 30-Hz charge exchange H^- source has been suspended so that maximum effort can be concentrated on modifications to improve Penning source performance and completion of the new source test facility.

04393

V. APPLIED PLASMA PHYSICS

A. Disparate Clump Approximation in Neoclassical Transport Theory

C. D. Boley and E. M. Gelbard, Applied Physics Division

Since most tokamak experiments show evidence of impurity ions with a number of charge states, a realistic transport theory must be capable of describing these situations. Within the context of neoclassical transport theory, expressions for the appropriate transport coefficients are now available.[1-4] Two problems, however, stand in the way of their implementation into 1-D codes. First, the computation of the transport coefficients themselves consumes a great deal of machine time; and second, given the transport coefficients, the number of diffusion equations that must be solved simultaneously becomes very large as additional charge states are taken into account.

We have developed a "disparate clump" approximation that is expected to be helpful in alleviating these problems. Within this approximation, the plasma is allowed to have any number of ion species, each with an arbitrary number of charge states, but the ion masses are assumed to be disparate. We have employed this approximation in two specific problems. First we have made use of it in calculating the classical Spitzer function (response of the distribution function to a parallel electric field) for a multiple ion plasma. Our motivation here is the fact that the neoclassical transport coefficients giving the pinch effect and bootstrap current require the Spitzer function as input.[1,5] These transport coefficients can now be readily computed. In the second application, we have obtained the transport coefficients of a multiple ion plasma in the Pfirsch-Schlüter regime. These have been reduced to closed analytic form. Furthermore, certain special features of the final expresions suggest a very efficient method of solving the associated 1-D diffusion equations. Regardless of the number of species, only five diffusion equations need be solved simultaneously.

---

1 S. P. Hirshman and D. J. Sigmar, *Phys. Fluids*, 20, p. 418 (1977).

2 S. P. Hirshman, *Phys. Fluids*, 20, p. 589 (1977).

3 E. M. Gelbard and S. P. Hirshman, *Phys. Fluids*, 21, p. 145 (1978).

4 C. D. Boley, "Summary of Neoclassical Transport Coefficients for a Multispecies, Mixed-Regime Tokamak Plasma," Argonne National Laboratory, ANL/FPP/TM-101 (December, 1977).

5 S. P. Hirshman and A. H. Boozer, "The Neoclassical Current in a Toroidally-Confined Multispecies Plasma," Princeton Plasma Physics Laboratory, PPPL-1409 (1977).

B. Spectroscopic Data for Cu-like Ions[†]

K. T. Cheng and Y.-K. Kim, Radiological and Environmental Research Division

To provide spectroscopic data for plasma diagnosis we computed from relativistic Hartree-Fock wavefunctions, wavelengths and transition probabilities for Cu-like ions. We present selected data on Mo^{13+}, Xe^{25+} and W^{45+}. These ions have one 4s electron in the outermost shell, and they are expected to show strong emission lines in hot plasma. Although emissions from the np (both j = 1/2 and 3/2) levels are expected to be intense, there are possibilities that other emissions listed in Tables V-1 through V-3 may also be intense if the upper levels are populated by collisions with plasma electrons of moderate energies. Excitations to optically allowed levels are favored by collisions with fast electrons, but forbidden levels are populated easily by slow electrons.

In Table V-4 we compare our wavelengths with those calculated by Cowan[1] and also with experimental data.[2,3] The excellent agreement (1% or better) supports our past experience[4] that the relativistic Hartree-Fock calculations provide reliable wavelengths for alkali-like configurations, i.e., one electron outside closed shells.

[†] Further details are given in: K. T. Cheng and Y.-K. Kim, "Spectroscopic Data for Cu-like Ions," Argonne National Laboratory, ANL/FPP/TM-109 (April, 1978).

[1] R. D. Cowan, "Spectra of Highly Ionized Atoms of Tokamak Interest," Los Alamos Scientific Laboratory, LA-6679-MS (1977).

[2] E. Hinnov, *Phys. Rev. A*, 14, p. 1533 (1976).

[3] J. Reader and N. Acquista, *Phys. Rev. Letters*, 39, p. 184 (1977).

[4] Y.-K. Kim and K. T. Cheng, to appear in *J. Opt. Soc. Am.*

Table V-1. Wavelengths, f Values and Transition Rates for Mo^{13+}

Transition[a]		λ (Å)	Dipole f	A(sec-1)
4s	4p*	4.231+02[b]	2.321-01	8.648+09
4s	4p	3.739+02	5.305-01	1.266+10
4s	5p*	8.425+01	3.902-02	3.667+10
4s	5p	8.333+01	5.834-02	2.802+10
4p*	4d*	2.425+02	8.938-01	5.069+10
4p*	5s	1.179+02	1.068-01	5.124+10
4p*	5d*	8.845+01	2.638-02	1.125+10
4p	4d*	2.623+02	8.453-02	8.196+09
4p	4d	2.588+02	7.726-01	5.129+10
4p	5s	1.224+02	1.225-01	1.091+11
4p	5d*	9.095+01	3.996-03	3.222+09
4p	5d	9.076+01	3.277-02	1.769+10
4d*	4f*	2.615+02	8.425-01	5.477+10
4d*	5p*	1.858+02	1.396-01	5.395+10
4d*	5p	1.814+02	2.564-02	5.199+09
4d*	5f*	1.130+02	7.420-02	2.586+10
4d	4f*	2.651+02	3.971-02	3.768+09
4d	4f	2.651+02	7.945-01	5.657+10
4d	5p	1.831+02	1.577-01	4.705+10
4d	5f*	1.136+02	3.761-03	1.944+09
4d	5f	1.136+02	7.495-02	2.905+10
4f*	5d*	2.977+02	1.127-01	1.272+10
4f*	5d	2.957+02	7.928-03	6.049+08
4f*	5g*	1.858+02	1.201+00	1.741+11
4f	5d	2.957+02	1.190-01	1.210+10
4f	5g*	1.858+02	3.337-02	6.447+09
4f	5g	1.858+02	1.168+00	1.806+11
5s	5p*	9.751+02	3.187-01	2.235+09
5s	5p	8.649+02	7.202-01	3.211+09
5p*	5d*	5.556+02	1.212+00	1.309+10
5p	5d*	5.991+02	1.153-01	2.142+09
5p	5d	5.908+02	1.051+00	1.339+10
5d*	5f*	5.984+02	1.196+00	1.485+10
5d	5f*	6.068+02	5.642-02	1.022+09
5d	5f	6.065+02	1.129+00	1.536+10
5f*	5g*	2.832+03	1.718-01	1.071+08
5f	5g*	2.840+03	4.759-03	3.936+06
5f	5g	2.834+03	1.670-01	1.110+08

a. Levels with asterisk denote $j=\ell-1/2$, e.g., 4p*=4p(1/2), 4p=4p(3/2).

b. $4.231+02=4.231\times10^{2}$, etc.

Table V-2. Wavelengths, f Values and Transition Rates for Xe^{25+}

Transition[a]		λ(Å)	Dipole f	A(sec-1)
4s	4p*	2.321+02[b]	1.733-01	2.145+10
4s	4p	1.732+02	4.745-01	5.275+10
4s	5p*	3.246+01	6.975-02	4.416+11
4s	5p	3.178+01	9.283-02	3.066+11
4p*	4d*	1.190+02	6.913-01	1.628+11
4p*	5s	4.083+01	9.073-02	3.630+11
4p*	5d*	3.294+01	1.077-01	3.311+11
4p	4d*	1.441+02	5.839-02	1.874+10
4p	4d	1.384+02	5.513-01	1.280+11
4p	5s	4.343+01	1.179-01	8.341+11
4p	5d*	3.461+01	1.591-02	8.859+10
4p	5d	3.445+01	1.308-01	4.902+11
4d*	4f*	1.306+02	5.035-01	1.313+11
4d*	5p*	5.526+01	1.043-01	4.556+11
4d*	5p	5.331+01	1.698-02	3.985+10
4d*	5f*	3.952+01	3.020-01	8.598+11
4d	4f*	1.357+02	2.308-02	8.356+09
4d	4f	1.350+02	4.654-01	1.277+11
4d	5p	5.414+01	1.081-01	3.689+11
4d	5f*	3.997+01	1.522-02	6.354+10
4d	5f	3.993+01	3.006-01	9.432+11
4f*	5d*	6.993+01	5.922-02	1.212+11
4f*	5d	6.928+01	4.030-03	5.601+09
4f*	5g*	5.284+01	1.191+00	2.133+12
4f	5d	6.946+01	6.115-02	1.127+11
4f	5g*	5.295+01	3.316-02	7.887+10
4f	5g	5.293+01	1.160+00	2.210+12
5s	5p*	4.975+02	2.361-01	6.363+09
5s	5p	3.745+02	6.333-01	1.506+10
5p*	5d*	2.592+02	9.468-01	4.701+10
5p	5d*	3.127+02	8.059-02	5.498+09
5p	5d	3.000+02	7.583-01	3.747+10
5d*	5f*	2.986+02	7.603-01	3.792+10
5d	5f*	3.112+02	3.483-02	2.399+09
5d	5f	3.086+02	7.037-01	3.696+10
5f*	5g*	7.846+02	1.799-01	1.462+09
5f	5g*	8.013+02	4.888-03	5.078+07
5f	5g	7.950+02	1.727-01	1.458+09

a. Levels with asterisk denote $j=\ell-1/2$, e.g., 4p*=4p(1/2), 4p=4p(3/2).

b. 4.231+02=4.231×10^2, etc.

Table V-3. Wavelengths, f Values and Transition Rates for W^{45+}

Transition[a]		λ (Å)	Dipole f	A (sec-1)
4s	4p*	1.249+02[b]	1.223-01	5.226+10
4s	4p	6.187+01	5.160-01	4.495+11
4s	5p*	1.221+01	9.861-02	4.415+12
4s	5p	1.166+01	9.064-02	2.224+12
4p*	4d*	4.919+01	6.136-01	8.456+11
4p*	5s	1.428+01	7.741-02	2.533+12
4p*	5d*	1.197+01	1.518-01	3.536+12
4p	4d*	8.217+01	3.782-02	3.736+10
4p	4d	7.196+01	3.964-01	3.404+11
4p	5s	1.616+01	1.338-01	6.835+12
4p	5d*	1.326+01	2.882-02	1.093+12
4p	5d	1.312+01	2.251-01	5.819+12
4d*	4f*	6.795+01	3.100-01	2.985+11
4d*	5p*	1.866+01	9.597-02	3.678+12
4d*	5p	1.741+01	1.174-02	2.582+11
4d*	5f*	1.432+01	4.836-01	1.049+13
4d	4f*	7.700+01	1.295-02	1.457+10
4d	4f	7.453+01	2.705-01	2.436+11
4d	5p	1.795+01	8.160-02	2.533+12
4d	5f*	1.468+01	2.514-02	7.776+11
4d	5f	1.463+01	4.894-01	1.144+13
4f*	5d*	2.061+01	3.578-02	8.427+11
4f*	5d	2.026+01	2.226-03	3.616+10
4f*	5g*	1.715+01	1.219+00	2.072+13
4f	5d	2.044+01	3.503-02	7.457+11
4f	5g*	1.728+01	3.408-02	7.612+11
4f	5g	1.725+01	1.192+00	2.137+13
5s	5p*	2.574+02	1.665-01	1.676+10
5s	5p	1.296+02	6.767-01	1.344+11
5p*	5d*	1.038+02	8.414-01	2.604+11
5p	5d*	1.724+02	5.254-02	1.179+10
5p	5d	1.507+02	5.474-01	1.072+11
5d*	5f*	1.516+02	4.912-01	9.509+10
5d	5f*	1.736+02	2.039-02	4.515+09
5d	5f	1.663+02	4.288-01	7.755+10
5f*	5g*	3.145+02	1.402-01	7.090+09
5f	5g*	3.416+02	3.569-03	2.041+08
5f	5g	3.300+02	1.299-01	6.365+09

a. Levels with asterisk denote j=ℓ-1/2, e.g., 4p*=4p(1/2), 4p=4p(3/2).

b. 4.231+02=4.231 × 10^2, etc.

Table V-4. Wavelengths (in Å) for Cu-like Ions

Ion	Transition	Present Work	Cowan[1]	Hinnov[2]	Reader and Acquista[3]
Mo^{13+}	$5s_{1/2} - 4p_{1/2}$	117.9			117.149
	$- 4p_{3/2}$	122.4			121.647
	$4s_{1/2} - 4p_{1/2}$	423.1	425	423.5	423.576
	$- 4p_{3/2}$	373.9	376	373.8	373.647
Xe^{25+}	$4s_{1/2} - 4p_{1/2}$	232.1	234.1	234.2	
	$- 4p_{3/2}$	173.2	174.3	173.9	
W^{45+}	$4s_{1/2} - 4p_{1/2}$	124.9	127.5		
	$- 4p_{3/2}$	61.87	61.2		

FPP AND FPP-RELATED DOCUMENTS AUTHORED BY ARGONNE PERSONNEL

M. A. ABDOU
"Important Aspects of Radiation Shielding for Fusion Reactor Tokamaks," Proceedings of Fifth International Conference on Reactor Shielding, Science Press, Princeton (1977) p. 501.

M. A. ABDOU, D. EHST, V. MARONI AND W. M. STACEY
"Impact of Major Design Parameters on the Economics of Tokamak Power Plants"
Presented at the IAEA Conference and Workshop on Fusion Reactor Design, Madison, Wisconsin, October 10-21, 1977.

M. A. ABDOU, J. N. BROOKS, C. DENNIS, D. A. EHST, K. EVANS, JR., R. KUSTOM, V. A. MARONI, R. MATTAS, J. NOREM, B. MISRA, D. L. SMITH, W. M. STACEY, JR., H. C. STEVENS AND L. R. TURNER
"Parametric Systems Analyses for Tokamak Power Plants"
Argonne National Laboratory, ANL/FPP/TM-97 (October, 1977).

C. D. BOLEY
"Practical Results of Neoclassical Transport Theory for a Multispecies, Mixed-Regime Tokamak Plasma"
Argonne National Laboratory, ANL/FPP/TM-101 (December, 1977).

J. N. BROOKS, D. EHST, S. D. HARKNESS, J. NOREM, H. STEVENS AND L. TURNER
"Resistive Requirements for the Vacuum Wall of a Tokamak Fusion Reactor"
Pres. at the Seventh IEEE Symposium on Engineering Problems of Fusion Research, Knoxville, Tennessee (October 25-28, 1977).

J. BROOKS, K. EVANS, JR., H. STEVENS, L. TURNER
"The Equilibrium Field Coil System for the Argonne EPR Design
Pres. at the Seventh IEEE Symposium on Engineering Problems of Fusion Research, Knoxville, Tennessee (October 25-28, 1977).

J. N. BROOKS, R. E. FUJA, R. L. KUSTOM AND W. F. PRAEG
"Energy Storage and Transfer System for Experimental Power Reactor"
Pres. at the Seventh IEEE Symposium on Engineering Problems of Fusion Research, Knoxville, Tennessee (October 25-28, 1977).

J. BROOKS, S. HARKNESS, J. JUNG, B. MISRA, A. MORETTI, J. NOREM AND H. STEVENS
"A Lower Hybrid Heating System for an Ignition Tokamak"
Pres. at the Seventh IEEE Symposium on Engineering Problems of Fusion Research, Knoxville, Tennessee (October 25-28, 1977).

J. N. BROOKS, R. L. KUSTOM AND W. M. STACEY, JR.
"Plasma Driving System Requirements for Commercial Tokamak Fusion Reactors"
Pres. at the Seventh IEEE Symposium on Engineering Problems of Fusion Research, Knoxville, Tennessee (October 25-28, 1977).

K. T. CHENG AND Y.-K. KIM
"Oscillator Strengths in Ag-Isoelectronic Sequence"
Bull. Am. Physical Society, 22 (1977) p. 1334.

R. G. CLEMMER AND W. F. CALAWAY
"Impact of Plasma Performance Parameters upon the Vacuum and Tritium System Design Requirements for Near-Term Tokamak Reactors,"
Presented at the IAEA Conference and Workshop on Fusion Reactor Design, Madison, Wisconsin, October 10-21, 1977.

R. G. CLEMMER, R. H. LAND AND V. A. MARONI
"Simulation of Large Scale Air Detritiation Operations by Computer Modeling and Bench-Scale Experimentation"
Pres. at the Seventh IEEE Symposium on Engineering Problems of Fusion Research, Knoxville, Tennessee (October 25-28, 1977).

R. G. CLEMMER, R. H. LAND, V. A. MARONI AND J. M. MINTZ
"Simulation of Large-Scale Air Detritiation Operations by Computer Modeling and Bench-Scale Experimentation"
Argonne National Laboratory, ANL/FPP-77-3 (November, 1977).

J. W. DAWSON, A. MORETTI, H. C. STEVENS AND K. THOMPSON
"Alternate Ohmic Heating Coil Arrangements for Compact Tokamaks
Pres. at the Seventh IEEE Symposium on Engineering Problems of Fusion Research, Knoxville, Tennessee (October 25-28, 1977).

S. K. DEY
"Numerical Studies of a Perturbed Iterative Scheme with Applications to Coupled Nonlinear Systems of Equations"
Argonne National Laboratory, ANL/FPP/TM-96 (1977).

D. EHST, K. EVANS AND W. M. STACEY, JR.
"A Systematic Survey of Tokamak Reactor Physics Design Parameters"
Argonne National Laboratory, ANL/FPP/TM-95 (October, 1977).

K. EVANS, JR.
"High β_t Equilibria in Tokamaks"
Argonne National Laboratory, ANL/FPP/TM-98 (November, 1977).

J. A. FASOLO
"Power and Gas Flow Models for Monoenergetic Neutral Beam Injectors"
Pres. at the Seventh IEEE Symposium on Engineering Problems of Fusion Research, Knoxville, Tennessee (October 25-28, 1977).

J. FASOLO, R. FUJA, J. JUNG, J. MOENICH, J. NOREM, W. PRAEG AND H. STEVENS
"A Neutral Beam System for an Ignition Tokamak"
Pres. at the Seventh IEEE Symposium on Engineering Problems of Fusion Research, Knoxville, Tennessee (October 25-28, 1977).

Y. GOHAR
"Tokamak Divertor Impact on the Toroidal Field Magnet and Vacuum System"
Pres. at the Seventh IEEE Symposium on Engineering Problems of Fusion Research, Knoxville, Tennessee (October 25-28, 1977).

S. D. HARKNESS, M. ABDOU, S. MAJUMDAR, V. MARONI, B. MISRA, B. CRAMER, J. DAVIS, D. DEFREECE AND D. KUMMER
"The Establishment of Alloy Development Goals Important to the Commercialization of Tokamak-Based Fusion Reactors"
Argonne National Laboratory, ANL/FPP/TM-99 and McDonnell Douglas Astronautics Company, MDCE-1743 (November, 1977).

S. D. HARKNESS, B. MISRA AND S. MAJUMDAR
"Thermal Stress and Creep Fatigue Limitations in First Wall Design"
Presented at the IAEA Conference and Workshop on Fusion Reactor Design, Madison, Wisconsin, October 10-21, 1977.

R. R. HEINRICH, L. R. GREENWOOD, G. R. ODETTE, H. FARRAR IV, R. DIERCKX
"Dosimetry Needs for the Magnetic Fusion Materials Program"
Proc. of the Second ASTM Euratom Symposium on Reactor Dosimetry, EPRI, Palo Alto, California, October 3-7, 1977.

M. A. HILAL, S-T. WANG, J. W. DAWSON AND J. D. GONZY
"Heat Transfer and Flow Characteristics of Liquid Helium in Narrow Channels"
Pres. at the Seventh IEEE Symposium on Engineering Problems of Fusion Research, Knoxville, Tennessee (October 25-28, 1977).

M. KAMINSKY
"Wall Erosion Phenomena in Controlled Fusion Devices"
Presented at the International Conference on Alternative Energy Sources, University of Miami, December 5-7, 1977.

A. R. KRAUSS AND D. M. GRUEN
"Relative Ion Sputtering Yield Measurements by Integration of Secondary Ion Energy Distribution Using a Retarding-Dispersive Ion Energy Analyzer"
Applied Physics, 14 (1977) p. 89-97.

R. L. KUSTOM, ET AL.
"Energy Storage and Transfer Systems for Tokamak Reactors"
Presented at the IAEA Conference and Workshop on Fusion Reactor Design, Madison, Wisconsin, October 10-21, 1977.

R. L. KUSTOM, R. B. WEHRLE, R. P. SMITH AND R. E. FUJA
"Argonne National Laboratory Energy Storage and Transfer Experimental Program"
Pres. at the Seventh IEEE Symposium on Engineering Problems of Fusion Research, Knoxville, Tennessee (October 25-28, 1977).

J. M. MINTZ, R. CLEMMER AND V. A. MARONI
"Tritium Handling Trade Studies and Design Options for the GA/ANL TNS"
Pres. at the Seventh IEEE Symposium on Engineering Problems of Fusion Research, Knoxville, Tennessee (October 25-28, 1977).

B. MISRA AND V. A. MARONI
"Thermal Hydraulic Analyses of Two Fusion Reactor First Wall/Blanket Concepts"
Pres. at the Seventh IEEE Symposium on Engineering Problems of Fusion Research, Knoxville, Tennessee (October 25-28, 1977).

W. F. PRAEG
"Protection of Neutral-Beam-Accelerator Electrodes from Spark Discharges"
Pres. at the Seventh IEEE Symposium on Engineering Problems of Fusion Research, Knoxville, Tennessee (October 25-28, 1977).

D. L. SMITH AND I. CHARAK
"Thermal Responses of Tokamak Reactor First Walls During Cycle Plasma Burns"
Pres. at the Seventh IEEE Symposium on Engineering Problems of Fusion Research, Knoxville, Tennessee (October 25-28, 1977).

R. SMITH
"Magnet Design for the TEPR OH Coil Homopolar Generator"
Argonne National Laboratory, ANL/FPP/TM-102 (December, 1977).

W. M. STACEY, JR., J. N. BROOKS AND K. EVANS, JR.
"Plasma Engineering Studies for the Tokamak Experimental Power Reactor"
Pres. at the Seventh IEEE Symposium on Engineering Problems of Fusion Research, Knoxville, Tennessee (October 25-28, 1977).

W. M. STACEY, JR., M. A. ABDOU, J. N. BROOKS, I. CHARAK, R. G. CLEMMER, J. DAWSON, K. EVANS, J. A. FASOLO, R. FUJA, S. D. HARKNESS, R. L. KUSTOM, V. A. MARONI, B. MISRA, J. NOEMICH, A. MORETTI, J. NOREM, W. F. PRAEG, D. L. SMITH, H. C. STEVENS, L. TURNER, S-T. WANG AND C. K. YOUNGDAHL
"Tokamak Experimental Power Reactor"
Presented at the IAEA Conference and Workshop on Fusion Reactor Design, Madison, Wisconsin, October 10-21, 1977.

W. M. STACEY, JR., M. A. ABDOU, J. N. BROOKS, I. CHARAK, R. G. CLEMMER, J. DAWSON, K. EVANS, J. A. FASOLO, R. FUJA, S. D. HARKNESS, R. L. KUSTOM, V. A. MARONI, B. MISRA, J. MOENICH, A. MORETTI, J. NOREM, W. F. PRAEG, D. L. SMITH, H. C. STEVENS, L. TURNER, S-T. WANG AND C. K. YOUNGDAHL
"Tokamak Experimental Power Reactor"
Argonne National Laboratory, ANL/FPP/TM-93 (November, 1977).

H. C. STEVENS, B. MISRA AND C. K. YOUNGDAHL
"Mechanical Design and Analysis for an EPR First Wall/Blanket/Shield System"
Pres. at the Seventh IEEE Symposium on Engineering Problems of Fusion Research, Knoxville, Tennessee (October 25-28, 1977).

SYSTEMS STUDIES PROJECT/ARGONNE NATIONAL LABORATORY
"ANL Parametric Systems Studies"
Argonne National Laboratory, ANL/FPP/TM-100 (November, 1977).

L. R. TURNER
"Limits on the Field of Ohmic Heating Solenoids Applied to a Tokamak TNS"
Pres. at the Seventh IEEE Symposium on Engineering Problems of Fusion Research, Knoxville, Tennessee (October 25-28, 1977).

L. R. TURNER AND M. A. ABDOU
"Computational Model for Superconducting Toroidal-Field Magnets for a Tokamak Reactor"
Pres. at the Seventh IEEE Symposium on Engineering Problems of Fusion Research, Knoxville, Tennessee (October 25-28, 1977).

L. R. TURNER, S-T. WANG, S. H. KIM, Y. C. HUANG AND R. P. SMITH
"Superconducting Magnet Systems for the ANL EPR Design"
Pres. at the Seventh IEEE Symposium on Engineering Problems of Fusion Research, Knoxville, Tennessee (October 25-28, 1977).

S-T. WANG, R. FUJA, S-H. KIM, R. L. KUSTOM, W. F. PRAEG, K. THOMPSON AND L. R. TURNER
"The Superconducting Ohmic-Heating System"
Pres. at the Seventh IEEE Symposium on Engineering Problems of Fusion Research, Knoxville, Tennessee (October 25-28, 1977).

S-T. WANG, S-H. KIM, W. F. PRAEG AND C. I. KRIEGER
"ANL Experimental Program for Pulsed Superconducting Coils"
Pres. at the Seventh IEEE Symposium on Engineering Problems of Fusion Research, Knoxville, Tennessee (October 25-28, 1977).

R. B. WRIGHT AND D. M. GRUEN
"Raman Scattering Study of Ion Bombardment Induced Amorphization of SiC"
Radiation Effects, 33 (1977) pp. 130-140.

Distribution for ANL/FPP-77-77

Internal:

M. Abdou
C. C. Baker
C. C. Bolta
J. Brooks
F. Cafasso
J. B. Darby
D. Ehst
K. Evans
J. Fasolo
E. Gelbard
L. Greenwood
D. M. Gruen, A. Krauss
S. Harkness
M. Kaminsky, S. Das, P. Dusza
Y. K. Kim
R. L. Kustom, W. Kim, W. Praeg, S-T. Wang
V. Maroni
F. Nolfi, B. Hall, H. Wiedersich
D. L. Smith
B. Ancker-Johnson
R. Avery
L. Burris, Jr.
E. J. Croke
S. A. Davis
P. R. Fields
B. R. T. Frost
P. F. Gustafson
R. V. Laney
R. L. Martin
M. V. Nevitt
E. N. Pettitt
E. G. Pewitt
D. C. L. Price
R. J. Royston
R. G. Sachs
W. K. Sinclair
C. E. Till
J. van Erp
R. S. Zeno
G. T. Garvey
A. B. Krisciunas
FP Program (20)
ANL Contract Copy
ANL Libraries (5)
TIS Files (5)

External:

DOE-TIC, for distribution per UC-20, plus -20a through -20g (406)
Manager, Chicago Operations Office
Chief, Chicago Patent Group
President, Argonne Universities Association
Applied Physics Division Review Committee:
  P. W. Dickson, Jr., Westinghouse Electric Corp.
  R. L. Hellens, Combustion Engineering, Inc.
  W. B. Loewenstein, Electric Power Research Inst.
  R. F. Redmond, Ohio State U.
  R. Sher, Stanford U.
  D. B. Wehmeyer, Detroit Edison
  S. A. Werner, U. Missouri
Chemical Engineering Division Review Committee:
  C. B. Alcock, U. Toronto
  R. C. Axtmann, Princeton U.
  J. T. Banchero, U. Notre Dame
  T. Cole, Ford Motor Co.
  P. W. Gilles, U. Kansas
  R. I. Newman, Allied Chemical Corp.
  G. M. Rosenblatt, Pennsylvania State U.
Chemistry Division Review Committee:
  J. Bigeleisen, U. Rochester
  W. H. Flygare, U. Illinois
  H. F. Franzen, Iowa State U.
  H. S. Gutowsky, U. Illinois

D. R. Herschbach, Harvard U.
E. L. Muetterties, Cornell U.
J. O. Rasmussen, Lawrence Berkeley Lab.
F. S. Rowland, U. California, Irvine
J. H. Wang, State U. New York, Buffalo

Components Technology Division Review Committee:
J. W. Dally, U. Maryland
W. E. Kessler, Commonwealth Associates
N. J. Palladino, Pennsylvania State U.
N. C. Rasmussen, Massachusetts Inst. Technology
M. A. Schultz, Pennsylvania State U.
A. Sesonske, Purdue U.
H. Thielsch, ITT Grinnell Corp.

Materials Science Division Review Committee:
G. S. Ansell, Rensselaer Polytechnic Inst.
R. W. Balluffi, Cornell U.
S. L. Cooper, U. Wisconsin
S. Doniach, Stanford U.
H. L. Falkenberry, Tennessee Valley Authority
C. Laird, U. Pennsylvania
D. Lazarus, U. Illinois
M. T. Simnad, General Atomic
A. R. C. Westwood, Martin Marietta Labs.

Physics Division Review Committee:
B. Bederson, New York U.
D. A. Bromley, Yale U.
W. L. Brown, Bell Telephone Labs.
R. Middleton, U. Pennsylvania
D. E. Nagle, Los Alamos Scientific Lab.
J. W. Negele, Massachusetts Inst. Technology
H. B. Willard, Case Western Reserve U.

Reactor Analysis and Safety Division Review Committee:
S. Baron, Burns and Roe, Inc.
W. Kerr, U. Michigan
M. Levenson, Electric Power Research Inst.
S. Levy, S. Levy, Inc.
R. B. Nicholson, Exxon Nuclear Co., Inc.
D. Okrent, U. California, Los Angeles

Solid State Science Division Review Committee:
C. P. Flynn, U. Illinois
D. M. Ginsberg, U. Illinois
K. L. Kliewer, Iowa State U.
G. A. Russell, U. Missouri

ZGS Complex Review Committee:
R. L. Cool, Rockefeller U.
V. W. Hughes, Yale U.
J. D. Jackson, U. California, Berkeley
W. Lee, Columbia U.
H. A. Neal, Indiana U.
J. L. Rosen, Northwestern U.
L. C. Teng, Fermi National Accelerator Lab.

N. Amherd, R. Scott, Electric Power Research Institute
J. Baublitz, C. Head, J. Neff, DOE/DMFE
R. Balzhiser, Electric Power Research Institute

D. Beard, F. Coffman, E. Ziurys, DOE/DMFE
Roger Boom, G. L. Kulcinski, C. W. Maynard, R. Conn, University of Wisconsin
S. Locke Bogart, DOE/DMFE
W. Briggs, D. Kummer, McDonnell-Douglas Company - East
S. J. Buchsbaum, Bell Telephone Laboratories, Inc.
G. A. Carlson, R. W. Werner, Lawrence Livermore Laboratory
R. A. Carruthers, Culham Laboratory
G. Casini, Commission of the European Community Joint Research Center, ITALY
Library, Centre de Recherches en Physique des Plasma, SWITZERLAND
J. A. Casazza, Stone & Webster Management Consultants, Inc.
R. Challender, United Kingdom Atomic Energy Authority
F. F. Chen, University of California
J. F. Clarke, DOE/DMFE
M. Clarke, Combustion Engineering
M. Collins, E. Golankiewicz, Engelhard Minerals & Chemicals Corp.
Librarian, Culham Laboratory
N. Anne Davies, R. Blanken, D. Ignat, J. Willis, DOE/DMFE
S. O. Dean, A. M. Sleeper, DOE/DMFE
J. F. Decker, G. J. Mischre, P. Stone, W. Dove, DOE/DMFE
D. Dingee, Battelle - Northwest Laboratory
W. E. Drummond, H. Woodson, University of Texas at Austin
A. M. Dupas, Centre d'Etudes Nucleaires, FRANCE
T. S. Elleman, North Carolina State University
W. L. Ellis, E. Oktay, DOE/DMFE
J. Feinstein, Varian Associates, Incorporated
S. Fernbach, Lawrence Livermore Laboratory
H. Finger, Center of Energy Systems
Bibliotheque, Service du Confinement des Plasmas, CEA, Fontenay-aux-Roses
H. K. Forsen, Exxon Nuclear Company, Inc.
J. S. Foster, Jr., TRW
T. K. Fowler, Lawrence Livermore Laboratory
H. P. Furth, Princeton Plasma Physics Laboratory
M. B. Gottlieb, Princeton Plasma Physics Laboratory
J. N. Grace, K. Moses, L. K. Price, DOE/DMFE
D. Grafstein, Exxon Research & Engineering Co.
R. A. Gross, Columbia University
G. Hansen, Convair Division/General Dynamics
A. F. Haught, United Technologies Research Center
N. Hershkowitz, K. E. Lonngren, W. R. Savage, University of Iowa
I. Grant Hedrick, Grumman Aerospace Corporation
A. Hill, L. Lidsky, Massachusetts Institute of Technology
R. A. Huse, Public Service Electric & Gas Company
H. Horwitz, General Electric Company
G. R. Ingram, DOE/DMFE
Library, FOM-Institut voor Plasma-Fysica, THE NETHERLANDS
Thermonuclear Library, Japan Atomic Energy Research Institute
E. E. Kintner, DOE/DMFE
H. Kouts, Brookhaven National Laboratory
A. Kolb, Maxwell Laboratories
W. B. Kunkel, University of California, Berkeley
Library, Kurchatov Institute of Atomic Energy, U.S.S.R.
Library, Laboratorio Gas Ionizata, ITALY
S. Hale Lull, Northeast Utility Service Company
R. Lengye, Bibliothek, Max-Planck-Institute fur Plasmaphysik
G. H. Miley, F. H. Southworth, R. Turnbull, University of Illinois

R. Meyerand, United Technologies Research Center
T. Ohkawa, General Atomic Company
R. E. Price, I. L. Sadowski, D. M. Priester, DOE/DMFE
S. Naymark, Nuclear Services Corporation
J. Purcell, General Atomic Company
R. Davidson, DOE/DMFE
D. R. Morgan, L. A. Berry, ORNL
D. Steiner, M. Roberts, ORNL
R. Raeder, Max-Planck-Institute fur Plasmaphysik
H. Dreicer, Los Alamos Scientific Laboratory
C. Rickard, General Atomic Company
K. H. Schmitter, Max-Planck-Institute fur Plasmaphysik
Z. Shapiro, Westinghouse Electric Corporation
M. N. Rosenbluth, Institute of Advanced Study, Princeton, New Jersey
W. M. Stacey, Jr., Georgia Institute of Technology
J. Williams, DOE/DMFE
P. Rose, North West Inc.
H. Willenberg, Battelle - Northwest Laboratory
K. Zwilsky, M. Cohen, E. Dalder, C. Finfgeld, T. Reuther, DOE/DMFE
D. Stekart, DOE